ATTACHMENT B: AREA OF REVIEW AND CORRECTIVE ACTION PLAN
40 CFR 146.84(b)
CTV VI

1. Document Version History

Version	Revision Date	File Name	Description of Change
1	7/31/2024	Att B – CTV VI AoR_CA_v1	Original Submission
2	8/26/2025	Att B – CTV VI AoR_CA_v2	Response to May 15, 2025 EPA Comments
3	11/21/2025	Att B – CTV VI AoR_CA_v3	Response to EPA Comments Received August 21, 2025.

2. Facility Information

Facility name: CTV VI

Facility contact: Faisal Latif, Storage Development Manager
(661) 763-6274, faisal.latif@crc.com

Location: CTV VI, Fresno County, CA
36.82, -120.53

3. Computational Modeling Approach

The computational modeling workflow begins with the development of a three-dimensional (3D) representation of the subsurface geology. It leverages well data (bottom and surface hole location, wellbore trajectory, well logs, etc.) and two-dimensional (2D)/3D seismic data for rendering structural surfaces into a geo-cellular grid, which also includes seismic information to understand faults and flow barriers. Attributes of the grid include porosity, permeability, and facies distributions of reservoir lithologies by subzone, as well as observed fluid contacts and saturations for each fluid phase. This geologic model is often referred to as a static model, as it reflects the reservoir at a single moment. Carbon TerraVault Holdings, LLC (CTV) licenses Schlumberger Petrel, industry-standard geo-cellular modeling software, for building and maintaining static models. The static model becomes dynamic in the computational modeler with the addition of the following:

- Fluid properties such as density and viscosity for carbon dioxide (CO_2), each hydrocarbon and water phase
- Liquid and gas relative permeability
- Capillary pressure data

- Proposed injection well completions, injection rates and injection pressure over the life of the project
- Field pressure history
- Fluid geochemical analysis
- Rock and fluid compressibility

All injection wells are constant-rate controlled subject to a maximum allowable injection pressure that is based on fracture gradient with a 90 percent safety factor. Additionally, for each injector, a separate single wellbore model was built using the multiphase well nodal analysis software PROSPER, developed by Petroleum Experts Ltd. PROSPER has been used extensively in CO_2 enhanced oil recovery (EOR) to model CO_2 injection wells. Simulation estimated reservoir pressure near each injector was used as an input for the well performance modeling. Nodal analysis helped design the optimal CO_2 injection system, including tubing size designed to handle the constant mass rate of injection per day over the life of the project. PROSPER modeling results are presented in **Appendix 4: Operational Procedures** (**Appendix 4**).

Results from the computational model are used to establish the area of review (AoR), the 'region surrounding the geologic sequestration project where underground sources of drinking water (USDWs) may be endangered by the injection activity' (EPA 75 FR 77230). In the case of the CTV VI storage project, the AoR encompasses the maximum areal extent of the CO_2 plume that was defined by 0.01 CO_2 global mole fraction cutoff at 100 years post-injection, and pressures great enough to endanger underground sources of drinking water (USDWs) are not anticipated outside the CO_2 plume footprint.

3.1 Model Background

Computational modeling was completed using Computer Modeling Group's (CMG's) Equation of State Compositional Simulator (GEM). GEM is capable of modeling EOR, chemical EOR, geomechanics, unconventional reservoirs, geochemical EOR, and carbon capture and storage. GEM can model the flow of three components (gas, oil and aqueous) and multi-phase fluids, as well as predict phase equilibrium compositions, densities, and viscosities of each phase. This simulator incorporates all the physics associated with handling of relative permeability as a function of interfacial tension (IFT), velocity, composition, and hysteresis. Computational modeling for the CO_2 plume used the Peng-Robinson Equation of State and the solubility of CO_2 in water is modeled by Henry's Law. The Peng-Robinson Equation of State establishes the properties of CO_2 over the pressures and temperatures of the model. Solubility of CO_2 in aqueous phase was modeled by Henry's Law as a function of pressure, temperature, and salinity.

The plume model defines the potential quantity of CO_2 stored and simulates lateral and vertical movement of the CO_2 to define the extent of the CO_2 plume and the pressure changes in the reservoir during and after injection which are used to define the AoR.

The simulator predicts the evolution of the CO_2 plume by:

- Incorporating complex reservoir geometry and wells and utilizing a full field static geological 3D characterization of the reservoir incorporating lithology, saturation, porosity, and permeability.
- Forecasting the CO_2 plume movement and growth by inputting the operating parameters into simulation (injection pressure and rates).
- Assessing the movement of CO_2 after injection ceases and allowing the plume to reach equilibrium, including pressure equilibrium and compositions in each phase.

CMG's GEM (CMG-GEM) software has been used in numerous CO_2 sequestration peer reviewed papers, including:

- Simulation of CO_2 EOR and Sequestration Processes with a Geochemical EOS Compositional Simulator (Nghiemw et al., 2004).
- Model Predictions via History Matching of CO_2 Plume Migration at the Sleipner Project, Norwegian North Sea (Zhang et al., 2014).
- Geomechanical Risk Mitigation for CO_2 Sequestration in Saline Aquifers. (Tran et al., 2009).

3.2 Site Geology and Hydrology

The structure within the project area is characterized by a gently dipping homocline with <2° dip to the southeast. In the northern San Joaquin Basin, the Domengine Formation is composed of lower shoreface sands, the Garzas Formation is composed of deltaic sands, and the Blewett and Tracy Formations are composed of deep water submarine fan deposits. These sands are encompassed by shale (confining zone and lower sealing zone described in **Attachment A: Narrative Report** [**Attachment A**]) as they grade laterally into slope shales and basin-plain shales. Over the project area, the Garzas sand quality is marginal and, as a result, is not currently a perforation target but is still considered part of the Injection Zone. The Domengine, Garzas, Blewett, and Tracy Formations outcrop along the western basin margin; however, the stratigraphic thinning and faulting associated with the marginal uplift and as the greater than 10-mile distance from the AoR to the outcrop edge effectively isolate the outcrop from the downdip reservoirs. No mapped faults extend to, lie within, or intersect the AoR in any way. The Injection Zone sands are present across the entire AoR, thinning slightly to the east (**Figure 3.1**).

The Injection Zone is bound above by both the Kreyenhagen Shale and the shales of the Santa Margarita Formation and below by the Sawtooth Shale. The Kreyenhagen Shale (Confining Zone) and shales of the Santa Margarita Formation act as barriers between the USDW and the Injection Zone. The Kreyenhagen Shale has an average gross thickness of 352 feet within the model boundary and ranges from 500 to 650 feet in the AoR. The Kreyenhagen Shale serves as a regional seal that was deposited during a major transgressive event in the Eocene and has very low matrix permeability as discussed in Section 3.4. The competence of the Kreyenhagen Shale in confining upward fluid movement from the Injection Zone is established by its historical performance as the regional seal for hydrocarbon accumulation in adjacent gas fields (e.g., Moffat Ranch, Gill Ranch).

The Class VI injection wells will target injection in the Domengine, Blewett, and Tracy Formations. No gas has been produced from these sands within the AoR; however, these formations are gas-bearing reservoirs at nearby fields such as Moffat Ranch, Gill Ranch, Merril Avenue, Ash Slough, and Cheney Ranch gas fields. Well data, open-hole well logs (**Figure 3.2**), core data and 2D seismic lines were used to define the subsurface geological characteristics of stratigraphy, lithology, and rock properties.

3.3 Model Domain

A static geological model developed with Schlumberger's Petrel software, commonly used in the petroleum industry for exploration and production, is the computational modeling input. It allows the user to incorporate seismic and well data to build reservoir models and visualize reservoir simulation results. Model domain information is summarized in **Table 3.1**.

The geo-cellular grid covers a 1,994 square mile model area, with model dimensions of approximately 48.6 miles by 41.0 miles, ensuring that the computational model is large enough to account for boundary condition effects. In order to capture CO_2 storage mechanisms and properly resolve near-injection well effects, grid refinements are used in the project area and around the seven proposed injectors. In the 144-square-mile region around the project area, the grid cells were refined to a size of 1,056 feet by 1,056 feet. Near each injector, a 25.6-acre region was further refined such that the grid cell size was 105.6 feet by 105.6 feet. As we move farther away from the project area, the grid cell dimensions are larger, with a maximum cell size of 5,280 feet by 5,280 feet at the model edges. These grid dimensions are designed to allow for adequate resolution of plume development, injection pressure requirements, and pressure changes in the reservoir. The model grid is aligned southeast to northwest (40-degree rotation) parallel to the depositional trend of the Injection Zones. Model boundaries were defined as open boundaries in the southeast edge, northeast edge, and northwest edge, as no significant faults or stratigraphic barriers exist. The southwest edge, however, was modeled as a closed boundary due to the stratigraphic pinchout, thinning, and faulting at the basin edge (**Figure 3.3**).

Preferential flow pathways are primarily caused by reservoir heterogeneity, especially for permeability. The current dynamic fluid flow model captures this heterogeneity by incorporating geologic property variability (facies, porosity, permeability) based on well logs. This variability is guided by realistic spatial trends (variograms) away from the wells. As a result, the model effectively captures preferential flow pathways within the reservoir.

The open-hole logs have a half-foot resolution and an average vertical cell height of 7.7 feet was used via proportional gridding over the model domain to generate grid layers as shown in **Figure 3.4**. This cell height provides the vertical resolution necessary to capture significant lithologic heterogeneity (sand versus shale), which helps to ensure accurate upscaling of log data and distribution of reservoir properties in the static model. **Figure 3.5** shows a comparison of open-hole log data and the associated upscaled logs for the SHAW_1-6 (04019060050000) well within the model boundary but just outside the AoR.

3.4 Facies, Porosity and Permeability

Wireline log data were acquired with measurements that include, but are not limited to, spontaneous potential, natural gamma ray, borehole caliper, compressional sonic, resistivity, neutron porosity, and bulk density.

Formation porosity is determined one of two ways: from bulk density using 2.65 grams per cubic centimeter (g/cc) matrix density as calibrated from core grain density and core porosity data, or from compressional sonic using 55.5 microseconds per foot (μsec/ft) matrix slowness and the Wyllie time average equation. The compaction coefficient (Hilchie, 1978) was calculated using a depth-dependent shale travel time.

Log-derived permeability is determined by applying a core-based transform that uses capillary pressure porosity and permeability along with clay values from X-ray diffraction (XRD) or Fourier transformed infrared (FTIR) analysis. Volume of clay is determined by spontaneous potential and is calibrated to core data. Core data from 16 wells of similar age formations (Eocene, Paleocene, and Late Cretaceous) in the Sacramento Basin and the Northern San Joaquin Basin were used to develop a permeability transform (**Figure 3.6**). The transform and core data are illustrated in **Figure 3.7**.

Porosity and volume of clay were distributed using sequential Gaussian simulation (kriging) within the static model and permeability was populated by applying the porosity-volume of clay-permeability transform at each cell.

For modeling purposes, facies are divided into sand and shale. Shale facies are defined as having a volume of clay greater than 30 percent and sand facies as having less than or equal to 30 percent volume of clay. While additional depositional facies within the sands are potentially present, the current petrophysical dataset suggests that these sands are adequately described by a single, clay dependent permeability transform (**Figure 3.7**).

Multiple realizations of facies distributions were calculated to capture the possible range of uncertainty. A random withholding exercise was implemented whereby 20 percent of wireline logs were randomly withheld from the model building process and compared to the property distribution from the remaining 80 percent. The base case facies distribution parameters were defined as the case with the lowest error on the withheld data population.

After facies distribution, cells with shale facies are deactivated in the simulation due to their low permeability. Within the sand facies, subfacies are handled implicitly by implementing the clay-dependent porosity-permeability transform described above. This allows sands with higher clay content to follow a lower permeability trend along a continuous transform.

Porosity and volume of clay are distributed independently within the sand facies using the same kriging parameters and methodology as the base case facies distribution. Permeability is calculated at each cell using the independently distributed porosity and volume of clay values.

Figures 3.8(a) and 3.8(b) show the porosity and permeability histograms for the Domengine, Garzas, Blewett, and Tracy Injection Zones. **Figure 3.9** shows the distribution of permeability and porosity in the static model.

3.5 Constitutive Relationships and Other Rock Properties

As no site-specific Domengine, Garzas, Blewett, and Tracy Injection Zones relative permeability data were available, data obtained from cores in the Winters Formation in the Union Island Gas field, which has a similar geologic age and depositional setting, were used for the computational simulation. Two samples from well SONOL_SECURITIES_6 (04077202090000) were used to normalize, average, and denormalize the relative permeability (see **Figure 3.6** for well location). The gas-water relative permeability Corey model was used to match the laboratory data (e.g., Honarpour et al., 1986).

Gas-water Corey model Gas:

$$k_{rgw}(s_g) = k_{rgwc}\left(\frac{s_g - s_{gc}}{1 - s_{wr} - s_{gc}}\right)^{n_g} \quad (1)$$

where S_g = current gas saturation
s_{gc} = critical gas saturation to water displacement, 0.05
k_{rgwc} = maximum gas relative permeability to water displacement, 0.32
n_g = gas relative permeability curvature to water displacement, 2.55

Gas-water Corey model Water:

$$k_{rwg}(s_w) = k_{rwgc}\left(\frac{s_w - s_{wr}}{1 - s_{wr} - s_{gc}}\right)^{n_w} \quad (2)$$

where S_w = current water saturation
s_{wr} = residual water saturation to gas displacement, 0.54, scale up to 0.25 during dynamic modeling
k_{rwgc} = maximum water relative permeability to gas displacement, 0.447
n_w = water relative permeability curvature to gas displacement, 3.10

Capillary pressure data were obtained from SONOL_SECURITIES_5 (04077201910000), which is located close to SONOL_SECURITIES_6 (see **Figure 3.6** for well locations). Two samples from the SONOL_SECURITIES_5 were tested by centrifuge using an air-brine system. Laboratory-tested capillary pressure was converted to reservoir conditions and normalized by the Leverett J-function methodology (Leverett, 1941). Leverett's method creates a dimensionless function which normalizes the capillary pressure curves from different rock types and removes the effect of porosity and permeability in effort to understand the behavior of the underlying pore structure. A single capillary pressure curve was then generated based on the average permeability and porosity.

As described in Section 3.4, there are two facies defined in the model: sand and shale, with shale facies being deactivated in the simulation. Therefore, only one set of relative permeability and capillary pressure curves was used. **Figures 3.10** shows the relative permeability curves used in the Base Case and sensitivity cases (Base Case, Case G, and Case H). **Figure 3.11** shows the capillary pressure curve used in the computational model.

During pre-operational tests, additional cores will be collected, more special core analysis will be acquired, and the model will be updated accordingly. Additionally, as discussed below, several sensitivity analyses have been conducted to investigate the uncertainty related to these parameters.

3.6 Mineralization

Previous studies into reactive transport modeling and geochemical reaction in CCS have shown that the amount of CO_2 trapped by mineralization reactions is extremely small over a 100-year post injection time frame (IPCC, 2005) for sandstone reservoirs. For the sake of computational efficiency and the minor expected effect on the AoR, reactive transport was not included as a part of the compositional simulation modeling.

Potential geochemical reactions of the Injection Zones, Confining Zone, and formation fluids with the injectate streams being considered were modeled using PHREEQC (ph-REdox-Equilibrium), the U.S. Geological Survey (USGS) geochemical modeling software. Details on the modeling procedure and results are provided in **Appendix 3: CTV VI Geochemical modeling** (**Appendix 3**). The modeling indicates, as expected, that as the formations are stable quartz and Feldspar dominated mineralogy, the effect of geochemical reactions with the injectate will be minor. Based on molar mass, there is a minimal net molar mass change: 2 to 6.8 percent in the Injection Zones. This is not expected to have a major impact on porosity or permeability in the Injection Zones or the Confining Zone.

3.7 Boundary Conditions

The following boundary conditions were applied to the model domain:

- The Injection Formations are bound above by the Kreyenhagen Shale and below by the Sawtooth Shale. The overlying Kreyenhagen Shale, which is continuous and present at an average thickness of 352 feet over the model domain, has low permeability, and has been shown to be a proven hydrocarbon seal in nearby gas fields, and was thus set as a no-flow boundary.
- The southeast, northeast, and northwest bounding conditions to the model are open, as no significant faults or stratigraphic barriers exist. The southeast and northeast boundaries were modeled with a pore volume multiplier based on regional sand and porosity mapping. The northwest boundary was modeled using a Carter-Tracy aquifer; aquifer properties are given in **Table 3.2**.
- The southwest boundary is set as a no-flow boundary due to the stratigraphic pinchout, thinning, and faulting associated with the uplift on the western margin.

3.8 Initial Conditions

Initial model conditions (start of CO_2 injection) of the Domengine, Garzas, Blewett, and Tracy Injection Zones are given in **Table 3.3,** including temperature, pressure, and salinity, along with their data sources. The temperature is set as variable with depth using a fixed surface temperature of 72.5ºF and a geothermal gradient of 0.012°F per foot, which was approximated from 248 logging run bottom-hole temperature recordings in and around the project area (**Figure 3.12(a)**). A fixed surface temperature of 72.5ºF was selected because it produced the best-fit line through the upper range of the bottom-hole temperature (BHT) data. Since BHT data from a single logging run must be corrected for circulation time the temperature gradient was aligned with the high side of the data (Bassiouni, 1994). The initial reservoir pressure was determined to be above hydrostatic with a pressure gradient of roughly 0.439 pounds per square inch per foot (psi/ft), which was approximated from RFT log data (**Figure 3.12(b)**). Salinity of 20,700 parts per million (ppm) was used for the Domengine, Garzas, and Blewett, and a salinity of 21,100 ppm was used for the Tracy, which was approximated from water analysis in the area as discussed in Section 2.8.2 of **Attachment A**.

3.9 Operational Information

Details on the injection operation are presented in **Table 3.4**. The anticipated injection temperature at the wellhead is 90°F. Injection wells were assumed to be perforated throughout the entire thickness of the injection zone being targeted. Further details are provided in **Attachment A** and **Appendix 4**.

Table 3.4 includes injector locations, injection rate, anticipated perforated interval, duration, and injection pressure during the project life. All injection wells are constant-rate controlled subject to a maximum allowable downhole injection pressure that is based on the fracture gradient with a 90 percent safety factor. The CO_2 injection rate for each injector well versus time is shown in **Figure 3.13**. The cumulative CO_2 injection at each injector well versus time is shown in **Figure 3.14**. Bottom-hole pressure (BHP) versus time for each injector well is shown in **Figure 3.15**. Near injector reservoir pressure versus time for each injector well is shown in **Figure 3.16**.

3.10 Fracture Pressure and Fracture Gradient

Fracture gradient and maximum allowable downhole injection pressure values are given in **Table 3.5**. A fracture pressure gradient of 0.80 psi/ft is assumed for the Injection Zones. Within the project AoR, there is no site-specific fracture pressure or fracture gradient for the Injection Zones. However, several wells in the project vicinity do have fracture gradient data, either in the Injection Zones or in formations of similar age and depth. A step-rate test (SRT) was performed in the HILMAR_WD2 well within the Domengine Formation with a resultant fracture gradient of 0.82 psi/ft. Seven additional wells in the vicinity have formation integrity tests (FITs) or leak-off tests (LOTs) performed at similar depth ranges to the project Injection and Confining Zones. A total of 11 tests from these wells average 0.825 psi/ft from tests in the depth range of 3,000 to 12,350 feet true vertical depth (TVD). See Figure 2.5-5 of **Attachment A** for the locations of

the wells. For the computational simulation modeling and well performance modeling, a fracture gradient of 0.8 psi/ft was assumed for all zones.

At this time, no fracture gradient information has been found for the Confining Zone. CTV will determine a site-specific fracture pressure for the Confining Zone as described in **Attachment I: Pre-Operational Testing Plan**.

CTV will ensure that the downhole injection pressure is below 90 percent of the Injection Zone fracture pressure, calculated at the top of the perforations in the injection wells (**Table 3.5**). CTV expects to operate the wells with a planned downhole injection pressure well below the maximum allowable injection pressure calculated using the fracture gradient and safety factor.

3.11 Time Steps

Adaptive time-stepping control was used during the computational simulation. The time step duration was between a minimum of 0.00001 day to maximum of 31 days.

3.12 Proposed Carbon Dioxide Stream

CTV expects the CO_2 stream to be sampled at the transfer point from the source and analyzed according to the analytical methods described in Table 4 of the Quality Assurance and Surveillance Plan (**Appendix 10**) and Table C-1 of the Testing and Monitoring Plan **(Attachment C)**.

For the purposes of geochemical modeling, CO_2 plume modeling, and well design, two injectate compositions were considered when determining how to perform the required assessment. These injectate compositions are shown in **Table 3.6** and described below.

- Injectate 1: A potential injectate stream composition from DAC or a pre-combustion source (such as a blue hydrogen facility that produces hydrogen using steam methane reforming process) or a post-combustion source (such as a natural gas fired power plant or steam generator). The primary impurity in the injectate is nitrogen.

- Injectate 2: A potential injectate stream composition from a biofuel capture source (such as a biodiesel plant that produces biodiesel from a biologic source feedstock) or from an oil and gas refinery. The primary impurity in the injectate is light-end hydrocarbons (methane and ethane).

Additional details that evaluate the injectate:

- Compatibility with planned material selection is presented in the Well Construction Plans (**Attachment G**).

- Compatibility with the reservoir formation and geochemistry is presented in **Appendix 3: Geochemical modeling**.

- Details on the evaluation of the injectate composition on the AoR and injection operations is presented in Section 4.2.1.

The results from the above-described work aligns with the expectations set forth in **40 CFR § 146.86** and **40 CFR § 146.82**, which require an assessment of injectate compatibility with well materials and formation geochemistry.

Table 3.7 provides the CO_2 specification that is the project basis of design. This proposed specification limit is derived from the injectate composition assessed for material selection and using a minimum concentration of 1 percent as the threshold.

The injectate falls within the modeled bounds presented in the permit application, thereby-

- Remaining compatible with the reservoir and confining zones, **40 CFR § 146.82(c)(3)**
- Remaining compatible with the selected well materials, satisfying **40 CFR § 146.86**
- Injection operations remain compliant with the assumptions used in the project application

As required in **Attachment C**, the composition of the CO_2 will be monitored during the operational life of the Project to confirm that the chemical composition and physical characteristics of the injectate are consistent with the well design standards and operating conditions of the Class VI permits. After receiving the injectate sample, CTV will conduct a thorough review and ensure that components of the injectate not included in **Table 3.7** do not affect the storage complex or well materials.

4. Computational Modeling Results

4.1 Predictions of System Behavior

Figure 4.1 and **Figures 4.2(a) through 4.2(g)** show the computational modeling results and development of the CO_2 plume at different time steps. The plume boundary is defined by a 0.01 CO_2 global mole fraction cutoff at 100 years post-injection, which results in a boundary that contains 99.99 percent of the total injected CO_2 mass for injection. This cutoff provides confidence that the corrective action well review and potential impact to USDWs is conservative and has been appropriately evaluated. **Figures 4.2(a) through 4.2(g)** display cross sections of the plume evolution for the base case scenario at each injection well location. The average reservoir pressure in the approximate CO_2 plume area vs. time for Domengine, Blewett, and Tracy zones are shown in **Figure 4.3(a)** and the maximum injection-induced pressure through time at the uppermost injection layer (directly below the top confining layer) is shown in **Figure 4.3(b)**.

As shown in **Figure 4.1**, the CO_2 extent is largely defined 20 years post-injection for the different Injection Zones. The majority of the CO_2 injectate (74 percent) remains as supercritical CO_2 at the end of the simulation, with the remaining portion of the CO_2 dissolving in the

formation brine over the simulated 100 years post-injection. **Figure 4.4** shows the cumulative storage for each of the mechanisms.

4.2 Model Sensitivity Analyses and Validation

In addition to the plume modeling, CTV performed a volumetric estimate of the storage capacity of our plume footprint using U.S. Department of Energy (DOE) methodology (Goodman et al., 2011), using distributions from our geomodel for the storage reservoir and CO_2 properties, and storage efficiency coefficients for a deltaic sandstone reservoir using the widely applicable storage efficiency coefficients from Gorecki et al. (2009). P50 probability represents a 50 percent chance that a specific outcome will be achieved or exceeded and the P50 estimate from this volumetric approach was 193 million metric tons (MMT), which is well over the estimate from our dynamic modeling, which gives us further confidence that our storage capacity estimate from the dynamic modeling is appropriate.

4.2.1 CO_2 Injectate Effect on Plume and pressure change

As discussed in Section 7.2 of **Attachment A**, two major types of injectate compositions were considered based on the source:

- Injectate 1: A potential injectate stream composition from DAC or a pre-combustion source (such as a blue hydrogen facility that produces hydrogen using steam methane reforming process) or a post-combustion source (such as a natural gas fired power plant or steam generator). The primary impurity in the injectate is nitrogen.
- Injectate 2: A potential injectate stream composition from a biofuel capture source (such as a biodiesel plant that produces biodiesel from a biologic source feedstock) or from an oil and gas refinery. The primary impurity in the injectate is light-end hydrocarbons (methane and ethane).

The compositional simulation model developed in CMG-GEM software was run for the two simplified injectate compositions, and their results were also compared against a 100 percent CO_2 injectate case. The cumulative volume, rate, and injection duration for all three cases were kept the same.

The Injection Zones CO_2 plume for Injectate 1 and Injectate 2 is consistent with the plume outline for 100 percent CO_2 injectate (**Figure 4.5**), with negligible difference among the three cases. The CO_2 plume outline was defined by a 0.01 global CO_2 mole fraction cutoff at 100 years post-injection for all three cases. The 100-year post end of injection plumes for the three cases are shown in **Figure 4.5.** The wells that fall within the CO_2 plume are the same for all three cases.

Additionally, the average pore volume weighted reservoir pressure within the approximate plume boundary for three Injection Zones was plotted for the three cases and was found to be very close, with a maximum difference of 4 pounds per square inch (psi) seen between the cases, as shown in **Figure 4.6**. Multiple scenarios were also run to test the effect of mixing Injectate 1 and Injectate 2 in different ratios on the plume shapes. As expected, because the resulting mixed

injectates were still high-purity CO_2 streams with impurity concentrations in between those of Injectates 1 and 2, the plume shapes for these scenarios were within the envelope represented by the end-point compositions.

In summary, there is minimal effect of the minor components on the CO_2 plume boundary for the proposed injectate compositions. As such, CTV's plume and AoR modeling for corrective action assessment is adequate for the expected injectate composition ranges. CTV will confirm that the properties of the injectate are consistent with the model inputs during pre-operational injectate sampling, and will do so for any additional sources. In addition, the AoR will be reviewed per Section 6, Reevaluation Schedule and Criteria.

4.2.2 Sensitivity Cases

The base model simulation case (base case) contains a realistic representation of the hydrogeologic structure with conservative assumptions about site conditions, making the base case suitable for delineating the AoR. A sensitivity analysis was performed to examine the effects of varying inputs that represent site conditions with the potential to significantly impact the simulation results. The sensitivity analysis scenarios are listed in **Table 4.1** and include permeability, porosity, phase trapping, relative permeability end points and shape, and capillary pressure. The sensitivity analysis is performed using 100 percent CO_2 injectate in all scenarios. Results from the sensitivity analysis are displayed graphically in **Figure 4.7 and 4.8**.

To quantify the results of the sensitivity analysis, the size of the CO_2 plume was measured as an area (using the 0.01 CO_2 global mole fraction cutoff at 100 years post-injection) and the changes are quantified as percentage changes compared with the base case. There are only two cases with a plume size change greater than 10 percent compared to the base case. Case C results in a +34.7 percent plume size change, corresponding to increasing the permeability transform by a multiplier of 3, which is a high-end increase in the system permeability. Case A showed a -12.1 percent plume size change, corresponding to a porosity multiplier of 1.24. In all the sensitivity cases, the resulting CO_2 plume boundaries are similar and do not overlie additional corrective action wells except for Case C. Case C would have the potential to add three corrective action wells within the plume.

Overall, based on these sensitivity analyses, the proposed base case is considered conservative. The sensitivity analysis provides confidence that the corrective action well review and assessment of the potential endangerment of the USDW based on the base case are conservative and have been appropriately evaluated. During pre-operational testing, the model will be updated and the AoR and corrective action wells list will be re-evaluated based on the additional site-specific data gathered.

4.3 AoR Delineation

AoR delineation consists of determining the outermost extent of the separate-phase CO_2 plume and area of elevated pressure (pressure front) that pose risk to USDWs during the lifetime of the project. Elevated pressure may pose a risk to USDWs due to the potential for brine leakage from the injection zone into a USDW through an existing conduit, such as an improperly abandoned

well. In most cases the AoR will at a minimum be defined by the CO_2 plume footprint and may be larger if the pressure front extends beyond the CO_2 plume. CTV VI used the risk-based AOR approach as documented in **Appendix 9: Risk-Based AoR Delineation** (**Appendix 9**).

Various methods are available to determine the pressure threshold value that defines the outermost extent of the pressure front. In general, these methods are used to define a pressure at which brine will leak upwards through an abandoned well, leak into a USDW, and endanger the USDW due to water quality impairment. Risk-based AoR delineation accounts for processes that inhibit brine leakage through abandoned wells (e.g., presence of the mud column) and processes that minimize potential USDW impacts from hypothetical brine leakage (e.g., dilution and attenuation in the USDW). Risk-based AoR delineation strategies are supported by the U.S. Environmental Protection Agency (EPA) *Class VI AoR and Corrective Action Guidance* (p. 42).

Appendix 9 risk-based AoR delineation consisted of modeling brine leakage under conservative assumptions and resulting salinity impacts to the lowermost USDW. Brine leakage and USDW salinity transport modeling used conservative assumptions and accepted methods to simulate (1) brine leakage through an abandoned well and (2) subsequent contaminant fate and transport within the lowermost USDW. Modeling indicated that the vast majority of brine leakage through a hypothetical abandoned well in the vicinity of the project would discharge to the Zilch Monitoring Zone (below the lowermost UDSW); therefore, brine leakage to the USDW would be negligible. Concomitantly, elevated salinity levels in the lowermost USDW are calculated to be negligible. These results were based on an assumed injection-zone pressure increase of 500 psi. CMG-GEM modeling results indicate that a pressure increase of this magnitude will not occur outside the boundary of the CO_2 plume (**Figure 4.3(b)**).

Based on these results, pressures great enough to endanger USDWs are not anticipated outside the CO_2 plume footprint, and the final AoR boundary was based on the extent of the CO_2 plume. **Figure 4.9** shows the AoR extent, injector locations, and proposed monitoring well locations. Details on the monitoring wells are discussed further in **Attachment C**.

5. Corrective Action

5.1 Tabulation of Wells within the AoR

Wells within the AoR are associated with oil and gas exploration. Nearby commercial discoveries of natural gas were developed from 1935 onward. As such, there are excellent records for wells drilled in the study area and no undocumented historical wells in the AoR are expected.

CTV accessed internal databases as well as California Geologic Energy Management Division (CalGEM) information to identify and confirm wells within the AoR (California Department of Conservation, 2024; CalGEM, 2024).

Table 5.1 provides counts of wellbores that penetrate the confining zone within the AoR by status and type, for each wellbore with a unique API-12 identifier. **Appendix 6** provides a

complete list of all wellbores by API-12 within the AoR. As required by **40 CFR 146.84(c)(2)**, the well table in **Appendix 6** describes each well's type, construction, date drilled, location, measured depth, completion record relative to the injection zones, record of plugging, and requirement for corrective action, if necessary.

5.2 Protection of USDWs

For the project area, CTV assessed USDW protection by evaluating all wellbores that penetrate the Confining Zone in the AoR. The corrective action assessment included the generation of detailed casing diagrams for each wellbore, review of all perforations, top of cement assessment for each casing string, and determination of cement plug depths. In portions of the wells that will be exposed to the injection zone or CO_2, additives will be incorporated into the cement blend to prevent corrosion and ensure containment of CO_2 within the reservoir.

Non-endangerment of USDWs will be ensured during all stages of the project.

5.3 Wells Penetrating the Confining Zone

For wells penetrating the Confining Zone, the depth of the Confining Zone was determined by interpretation of open-hole well logs in conjunction with the deviation survey. Two wells in the AoR penetrate the Confining Zone. These wells also penetrate the Injection Zone. Both wells lie inside the CO_2 plume boundary and will be re-abandoned prior to injection.

5.4 Corrective Action Assessment of Wells in AoR

The two wells in the AoR were drilled as oil and gas exploration wells and determined to be dry holes (no hydrocarbon present), which resulted in abandonment of the open-hole section with a cement plug set across the surface casing and above the USDW. CTV will re-abandon these wells prior to injection to ensure that confinement is reestablished. A map with these wells is shown in **Figure 5.1**, and the table of wells in **Appendix 6** provides well information pursuant to **40 CFR §146.84(c)(2)**. Details of the abandonment procedures for these wells are provided in **Appendix 7** and **Appendix 8**.

5.5 Plan for Site Access

CTV has obtained surface access rights for the duration of the project.

5.6 Corrective Action Schedule

The two wells that fall in the AoR will be re-abandoned prior to injection. CTV will ensure that CO_2 is confined to the injection zones within the AoR, protecting the overlying USDW and ensuring confinement.

Through time, if the plume development is not consistent with the predicted results, computational modeling will be updated to reassess the AoR. In this event, any new wells in the updated AoR will be subject to the Corrective Action Plan and will be remediated if necessary.

6. Reevaluation Schedule and Criteria

6.1 AoR Reevaluation Cycle

CTV will reevaluate the AoR at a minimum every five years during the injection and post-injection phases, as required by **40 CFR 146.84 (e)**.

Simulation study results will be reviewed when operating data is acquired. Preparation of necessary operational data for the review includes injection rates and pressures, CO_2 injectate concentrations, and monitoring well information (storage reservoir and overlying monitoring intervals).

Dynamic operating and monitoring data that will be incorporated into future reevaluation will include:

1. Pressure data from monitoring wells that constrain and define plume development.
2. CO_2 content/saturation from monitoring wells. These data may be acquired with direct aqueous measurements and cased hole log results that will constrain and define plume development.
3. Injection pressures and volumes. The injection pressures and volumes in the computational model are maximum values. If the actual rates are lower than expected, the plume will develop at a slower rate than expected and be reflected in the pressure and CO_2 concentration data in 1 and 2 above.
4. A review of the full suite of water quality data collected from monitoring wells in addition to CO_2 content/saturation to evaluate the potential for unexpected reactions between the injected fluid and the rock formation.
5. Review and submission of any geologic data acquired since the last modeling effort, including any additional site characterization performed for future injection wells.
6. Reevaluation modeling results will be compared with the most recent modeling (i.e., from the most recent AoR reevaluation). A report describing the comparison of the modeling results will be provided to EPA with a discussion on whether the results are consistent.
7. Description of the specific actions that will be taken if there are discrepancies between monitoring data and prior modeling results (e.g., remodel the AoR, update all project plans, perform additional corrective action if needed, and submit the results to EPA).

The reevaluated results will be compared to the original results to understand dynamic inputs affecting plume development and static inputs that would impact injectivity and storage capacity. Discrepancies between the initial and reevaluated models may be due to static reservoir properties such as permeability, sand continuity, and porosity or other input parameters. Although the AoR has been fully delineated, all inputs to both the static and dynamic model will be reviewed.

As needed, CTV will review all of the plans that are impacted by a potential AoR increase such as corrective action and emergency and remedial response. For corrective action, all wells

potentially impacted by a changing AoR will be addressed immediately. Updates to the Testing and Monitoring Plan may include the addition of new USDW monitoring wells or additional plume and pressure front monitoring.

6.2 Triggers for AoR Reevaluations Prior to the Next Scheduled Reevaluation

An ad-hoc reevaluation prior to the next scheduled reevaluation will be triggered if any of the following occur:

- Changes in pressure or injection rate that are unexpected and outside three standard deviations from the average will trigger a new evaluation of the AoR.
- Difference between the computation modeling and observed plume development:
  - Unexpected changes in fluid constituents or pressure outside the zones of injection that are not related to well integrity.
  - Reservoir pressure increase versus injected volume is inconsistent with computational modeling results with a variance > ±10 percent from the base case simulation.
  - Any other activity prompting a model recalibration.
- Seismic monitoring anomalies within 2 miles of the injection well that are indicative of:
  - The presence of faults near the Confining Zone that indicates propagation into the Confining Zone.
  - Events reasonably associated with CO_2 injection that are greater than M3.5.
- Exceeding 90 percent of the geologic formation fracture pressure in any injection or monitoring wells.
- Detection of changes in shallow groundwater chemistry (e.g., a significant increase in the concentration of any analytical parameter that was not anticipated by the AoR delineation modeling).
- Initiation of competing injection projects within the same injection formation within a 1-mile radius of the injection well (including when additional CTV injection wells come online).
- A significant change in injection operations, as measured by wellhead monitoring.
- Significant land-use changes that would impact site access.
- Any other activity prompting a model recalibration.

CTV will discuss any such events with the UIC Program Director as soon as possible to determine if an AoR reevaluation is required. If an unscheduled reevaluation is triggered, CTV will perform the steps described at the beginning of this section of the plan within six months for the triggering event.

References

Bassiouni, Z. 1994. Theory, Measurement and Interpretation of Well Logs. Textbook Series, Vol. 4, Society of Petroleum Engineers (SPE).

California Department of Conservation. 2024. Geologic Energy Management Division's Well Statewide Tracking and Reporting System WellSTAR. https://wellstar.conservation.ca.gov

California Department of Conservation. Geologic Energy Management Division's (CalGEM), 2024. Online mapping application Well Finder. https://maps.conservation.ca.gov/doggr/wellfinder

IPCC, 2005 – Bert Metz, Ogunlade Davidson, Heleen de Coninck, Manuela Loos and Leo Meyer (Eds.) Cambridge University Press, UK. pp 431. Available from Cambridge University Press, The Edinburgh Building Shaftesbury Road, Cambridge CB2 2RU ENGLAND. https://www.ipcc.ch/report/carbon-dioxide-capture-and-storage/

Goodman, A., A. Hakala, G. Bromhal, D. Deel, T. Rodosta, S. Frailey, M. Small, D. Allen, V. Romanov, J. Fazio, N. Huerta, D. McIntyre, B. Kutchko, and G. Guthrie. 2011. U.S. DOE methodology for the development of geologic storage potential for carbon dioxide at the national and regional scale. *International Journal of Greenhouse Gas Control* 5(4): 952-965. ISSN 1750-5836, https://doi.org/10.1016/j.ijggc.2011.03.010.

Gorecki, C.D., J.A. Sorensen, J.M. Bremer, D.J. Knudsen, S.A. Smith, E.N. Steadman, and J.A. Harju. 2009. Development of storage coefficients for determining the effective CO_2 storage resource in deep saline formations. Paper presented at the SPE International Conference on CO_2 Capture, Storage, and Utilization, San Diego, California, USA, November 2009. doi: https://doi.org/10.2118/126444-MS

Honarpour, M., L. Koederitz, and A. H. Harvey. 1986. Relative Permeability of Petroleum Reservoirs. CRC Press. https://doi.org/10.1201/9781351076326

Hilchie, D.W. 1978. *Applied open-hole log interpretation*.

Leverett, M.C. 1941. Capillary Behavior in Porous Solids. *Trans.* 142. 152–169. https://doi.org/10.2118/941152-G

Nghiemw, L., A. Shrivastavar, B. Kohse, and P. Sammon. 2004. Simulation of CO_2 EOR and sequestration processes with a geochemical EOS compositional simulator. Paper presented at the Canadian International Petroleum Conference, Calgary, Alberta, June 2004. doi: https://doi.org/10.2118/2004-051

Tran, D., V. Shrivastava, L. Nghiem, and B. Kohse. 2009. Geomechanical risk mitigation for CO_2 sequestration in saline aquifers. Paper presented at the SPE Annual Technical Conference and Exhibition, New Orleans, Louisiana, October 2009. doi: https://doi.org/10.2118/125167-MS

Zhang G., L. Peng, and Z. Chen. 2014. Model predictions via history matching of CO_2 plume migration at the Sleipner Project, Norwegian North Sea. *Energy Procedia* 63: 3000-3011. ISSN 1876-6102, https://doi.org/10.1016/j.egypro.2014.11.323.

Figures

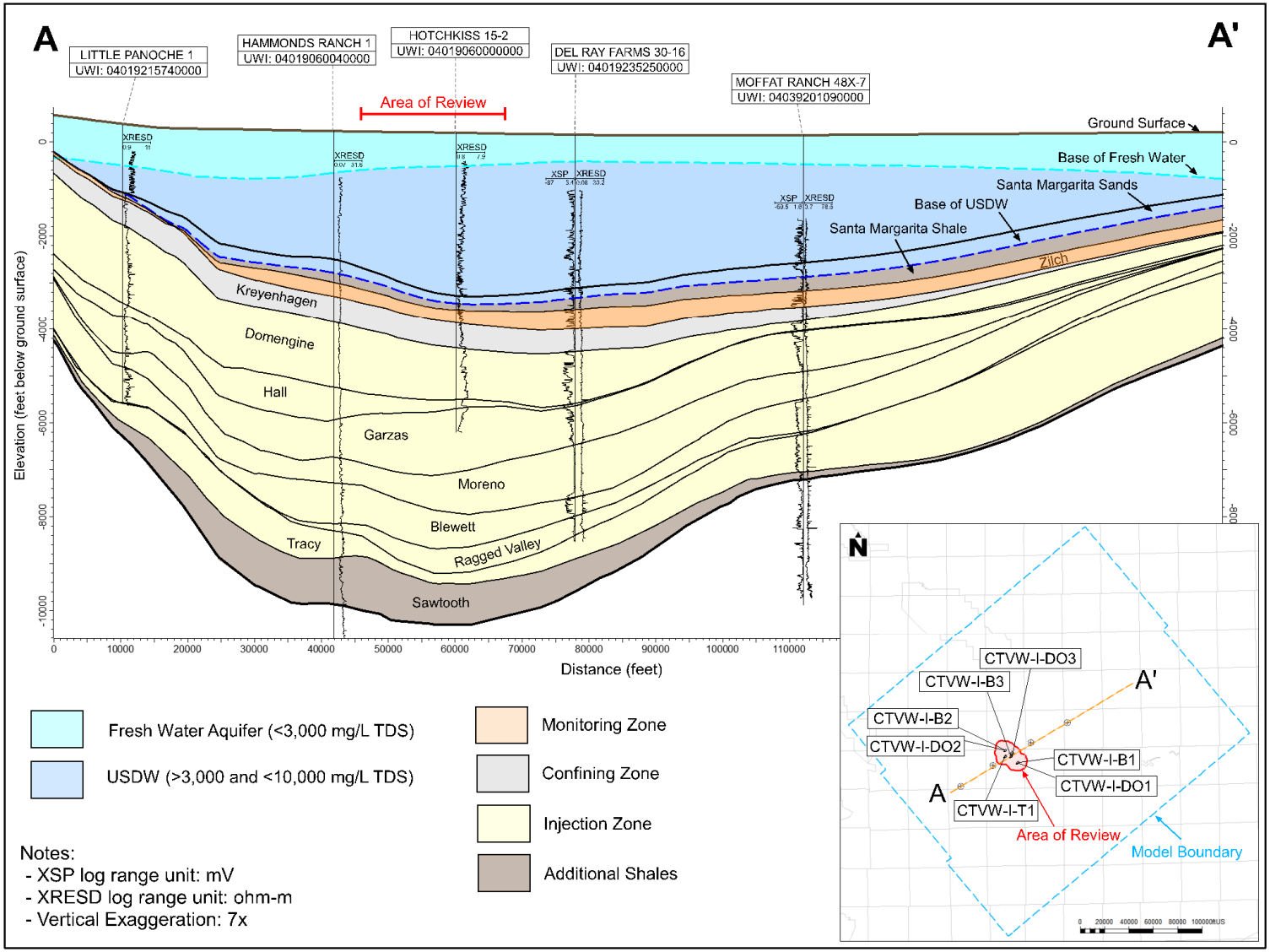

Figure 3.1. Cross section showing stratigraphy and lateral continuity of major formations across the AoR.

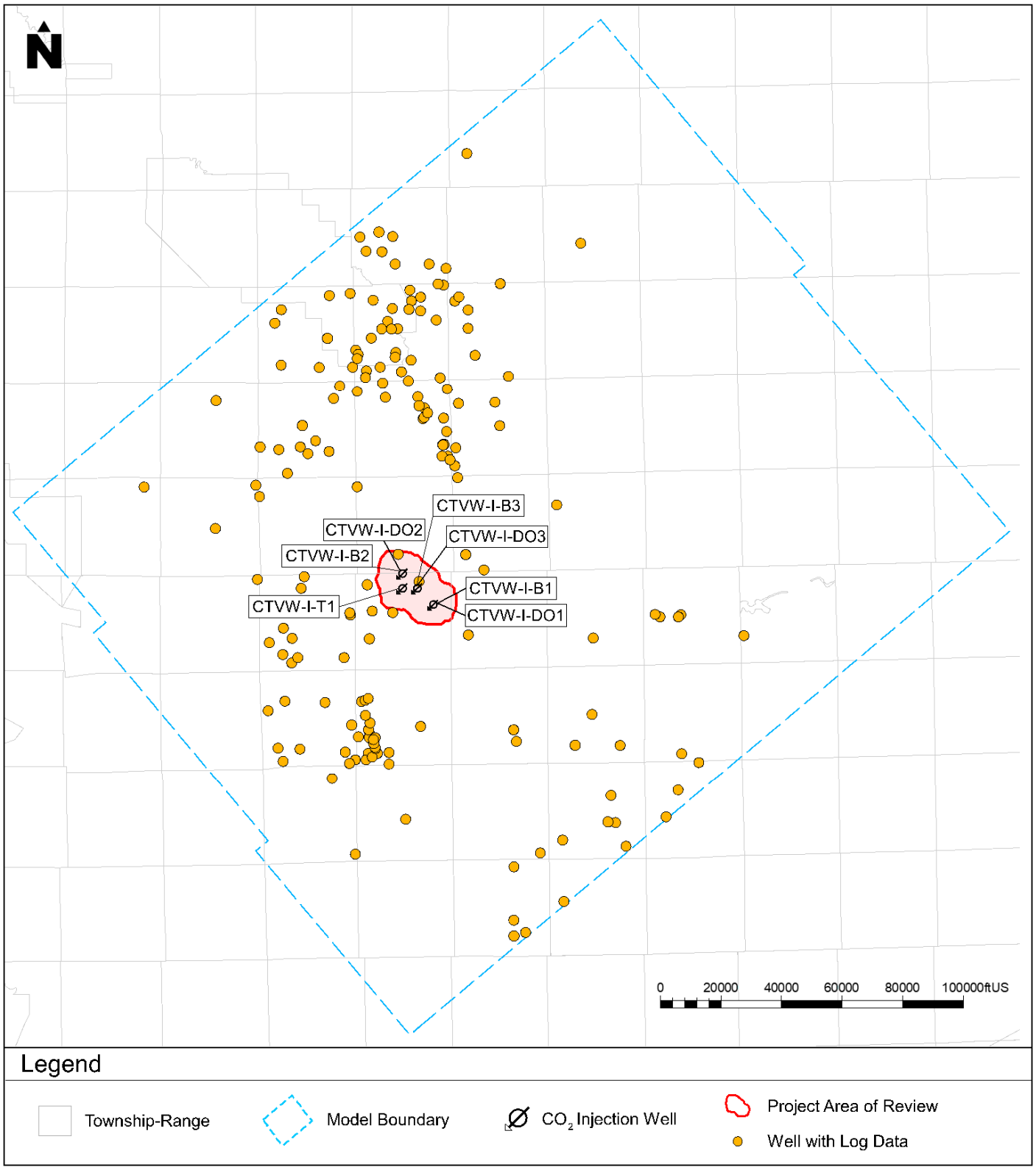

Figure 3.2. Location of wells with open-hole log data used to develop static and computational models.

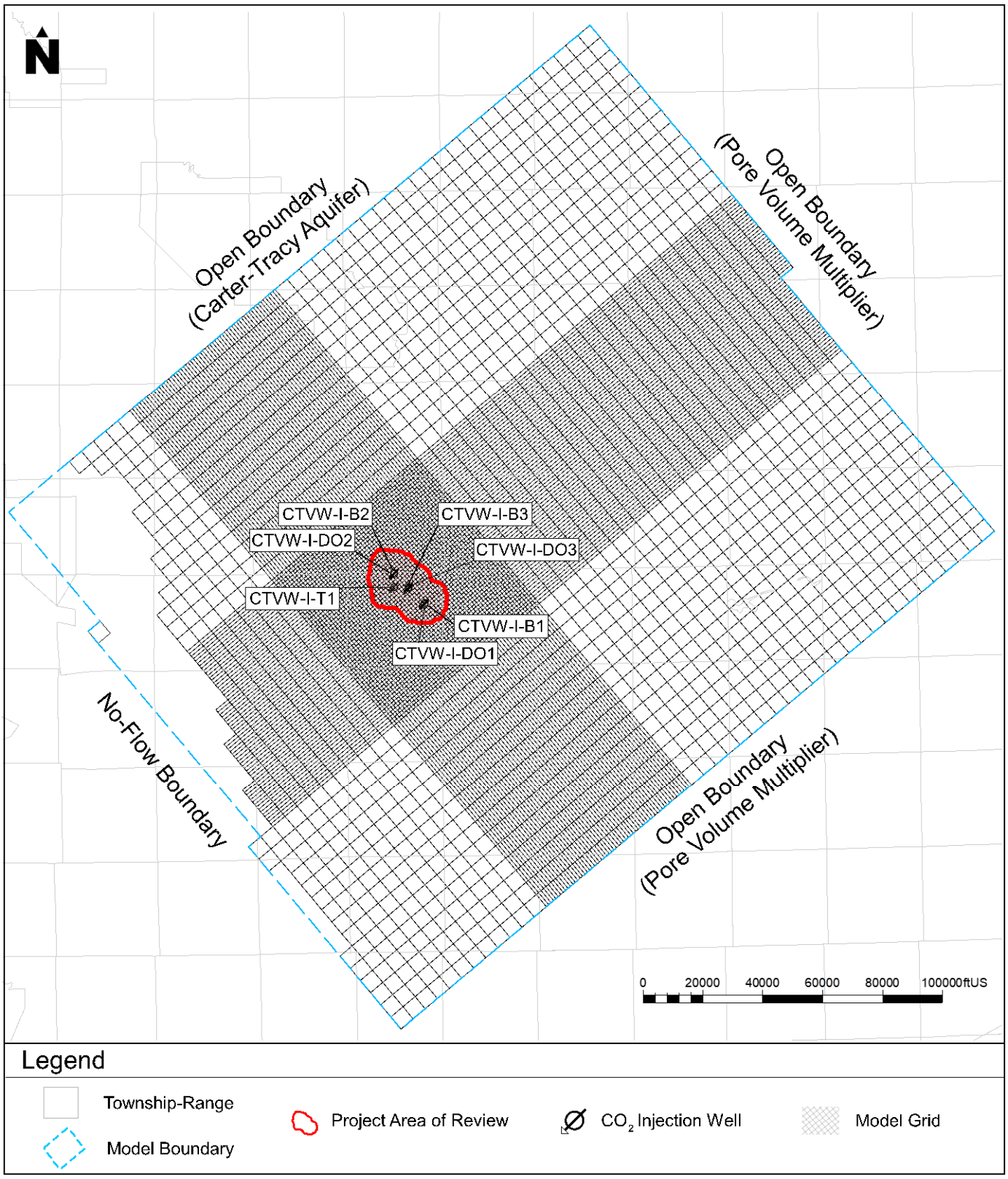

Figure 3.3. Plan view of model boundary and geo-cellular grid used to define the CO_2 plume extent and associated AoR.

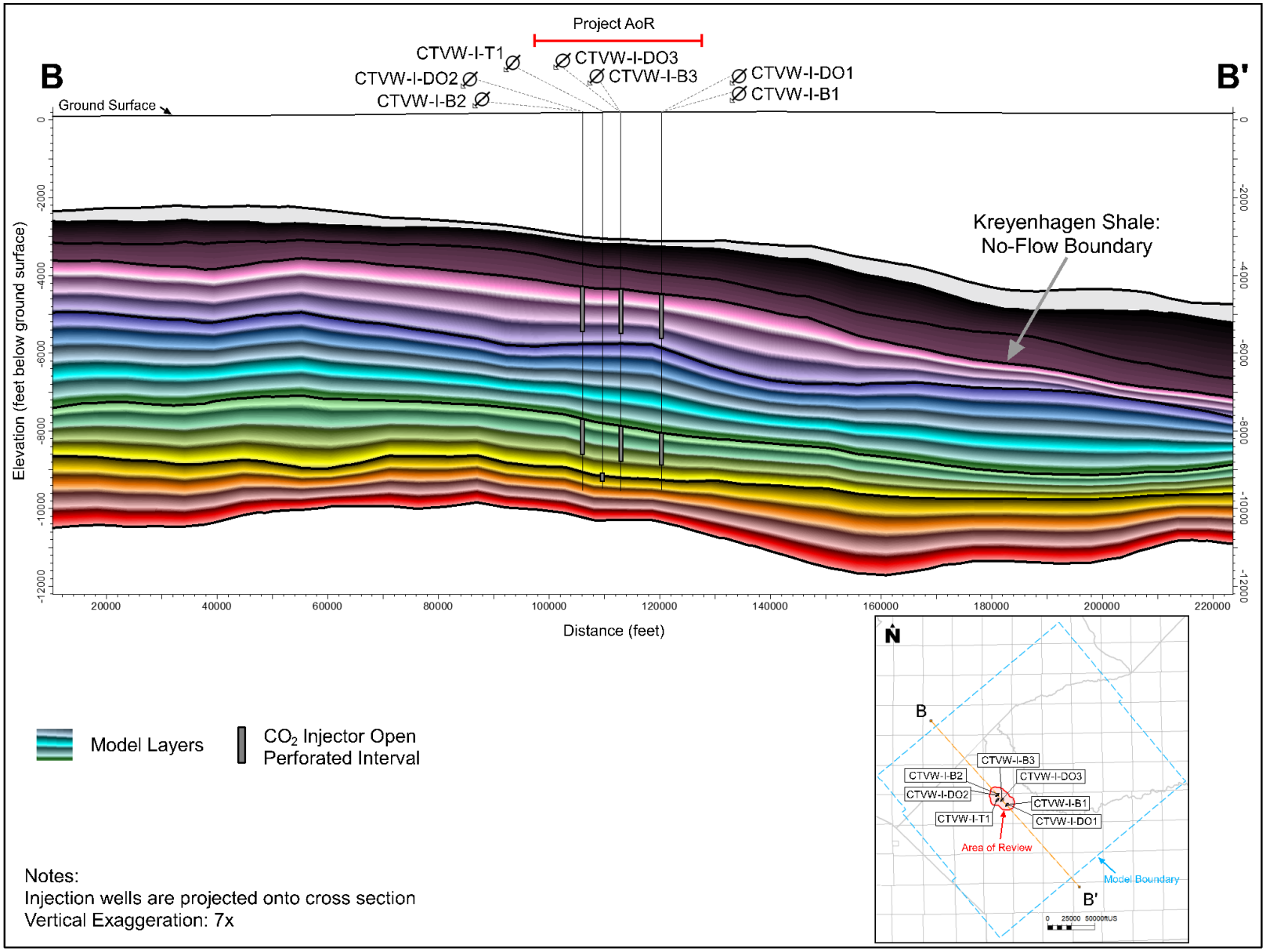

Figure 3.4. Static model grid layering of Injection Zone formations.

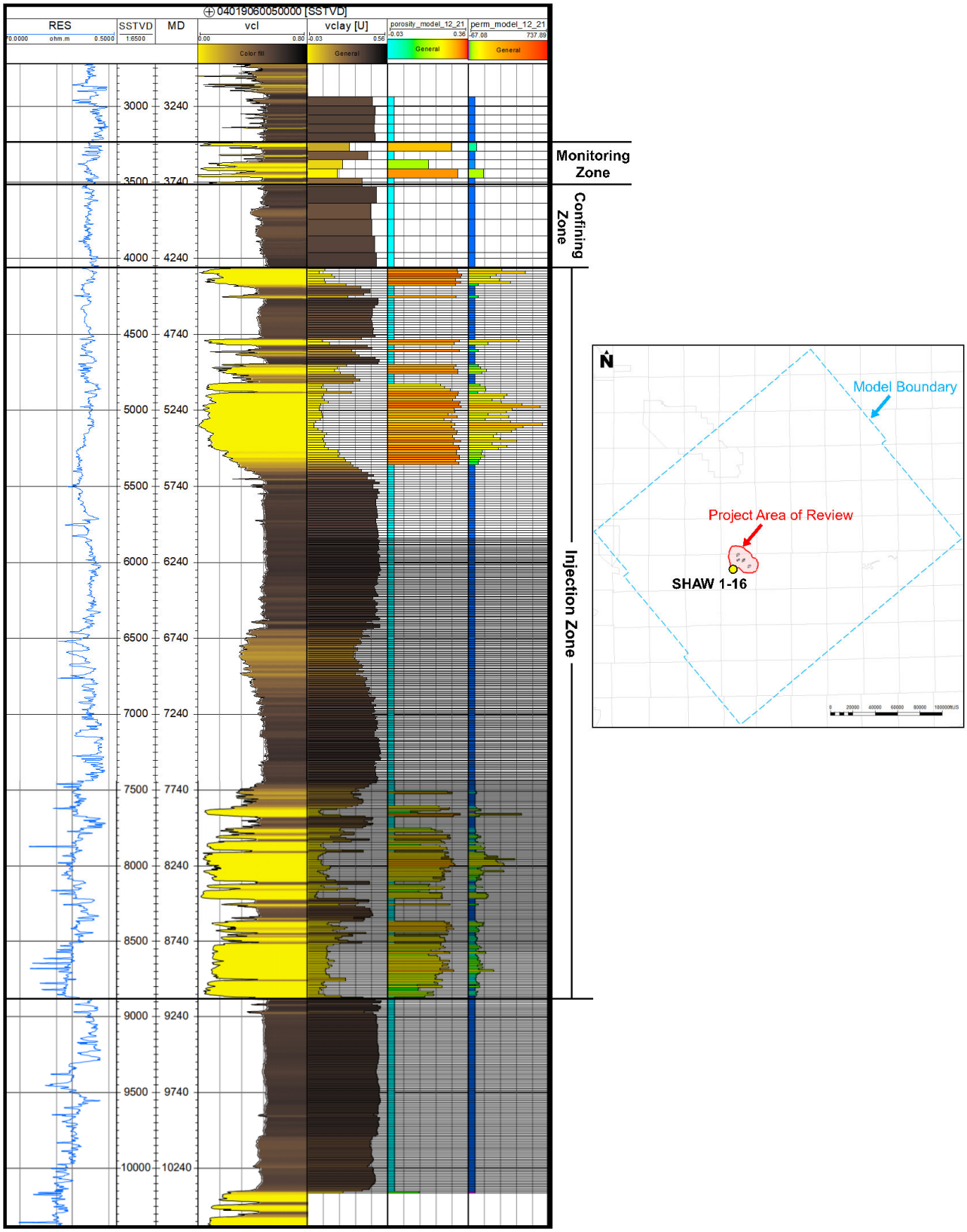

Figure 3.5. Well "SHAW_1-16" upscaled logs vs. open-hole logs.

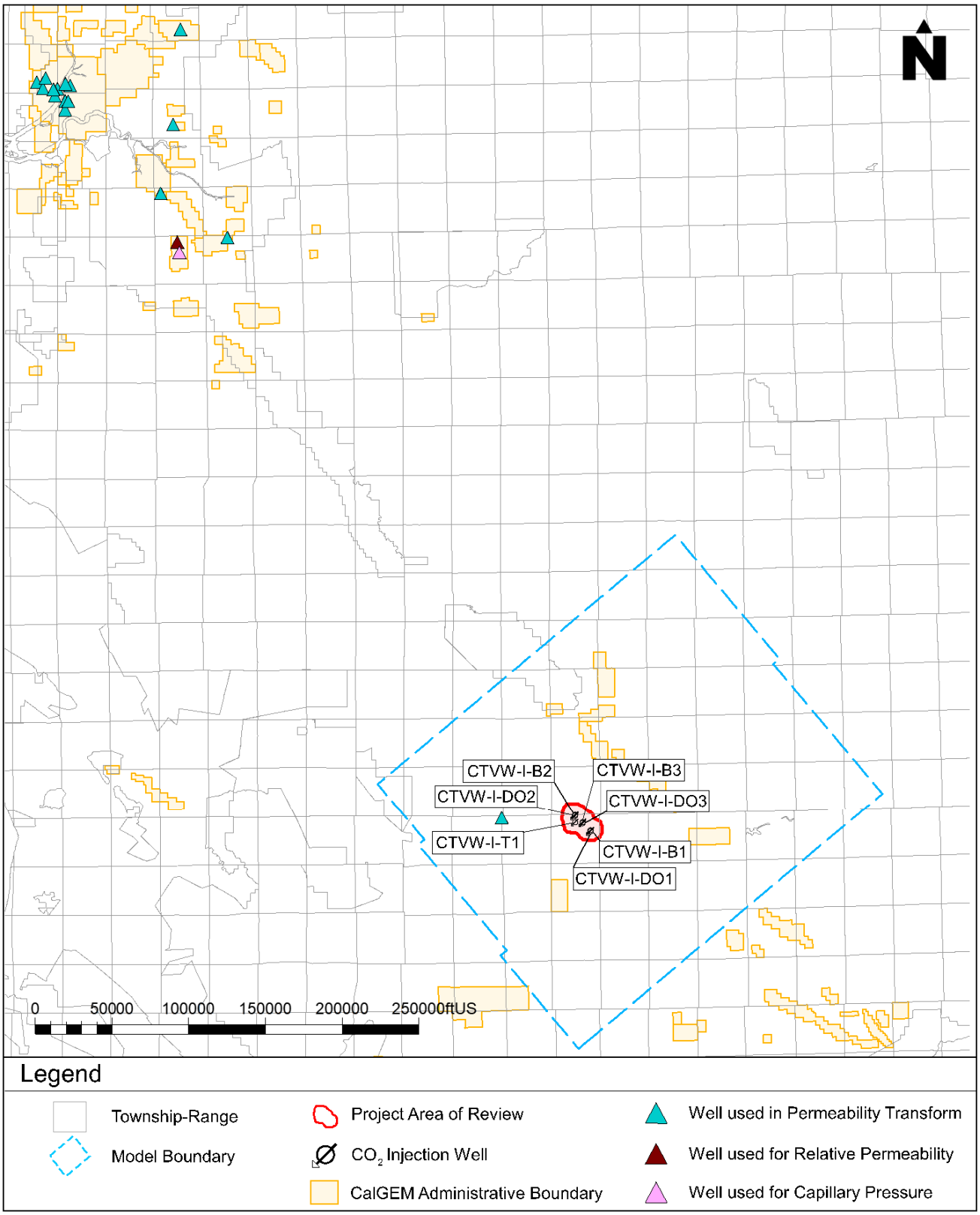

Figure 3.6. Location of wells with core data used for permeability transform and constitutive relationships

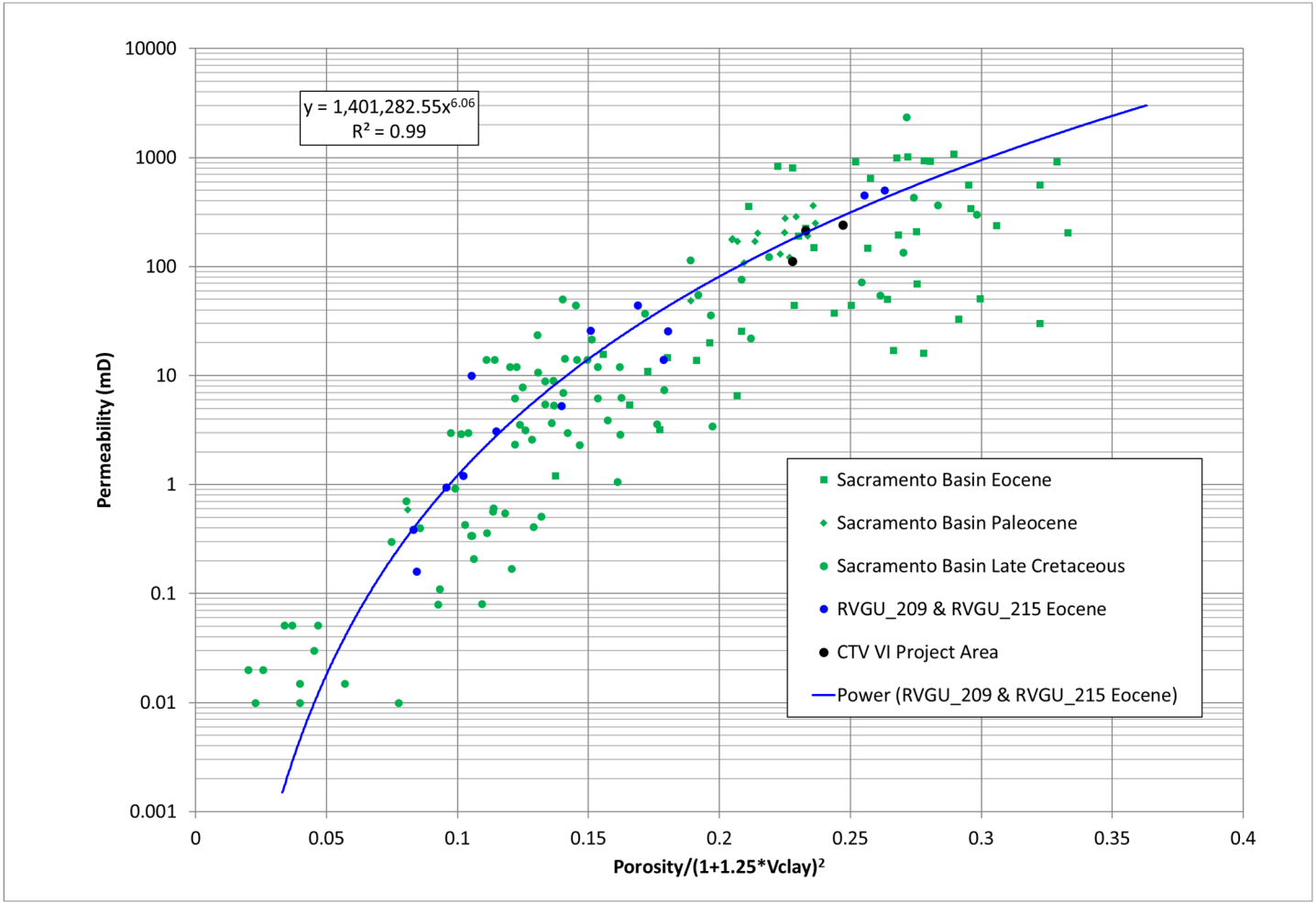

Figure 3.7. Permeability transform for CTV VI Injection zones. The blue data points are from two wells in Rio Vista gas field (RVGU_209 & RVGU_215) and are the basis for the permeability transform. Additional Core data from the Sacramento basin is also shown in green, with circles corresponding to Late Cretaceous age rock, diamonds corresponding to Paleocene age rock, and squares corresponding to Eocene age rock. The black data points are core from a well specific to the CTV VI model area. Data shown is limited to those core data points representing sand, with a clay volume from XRD of less than 25% clay and exclude any percussion sidewall derived permeability values.

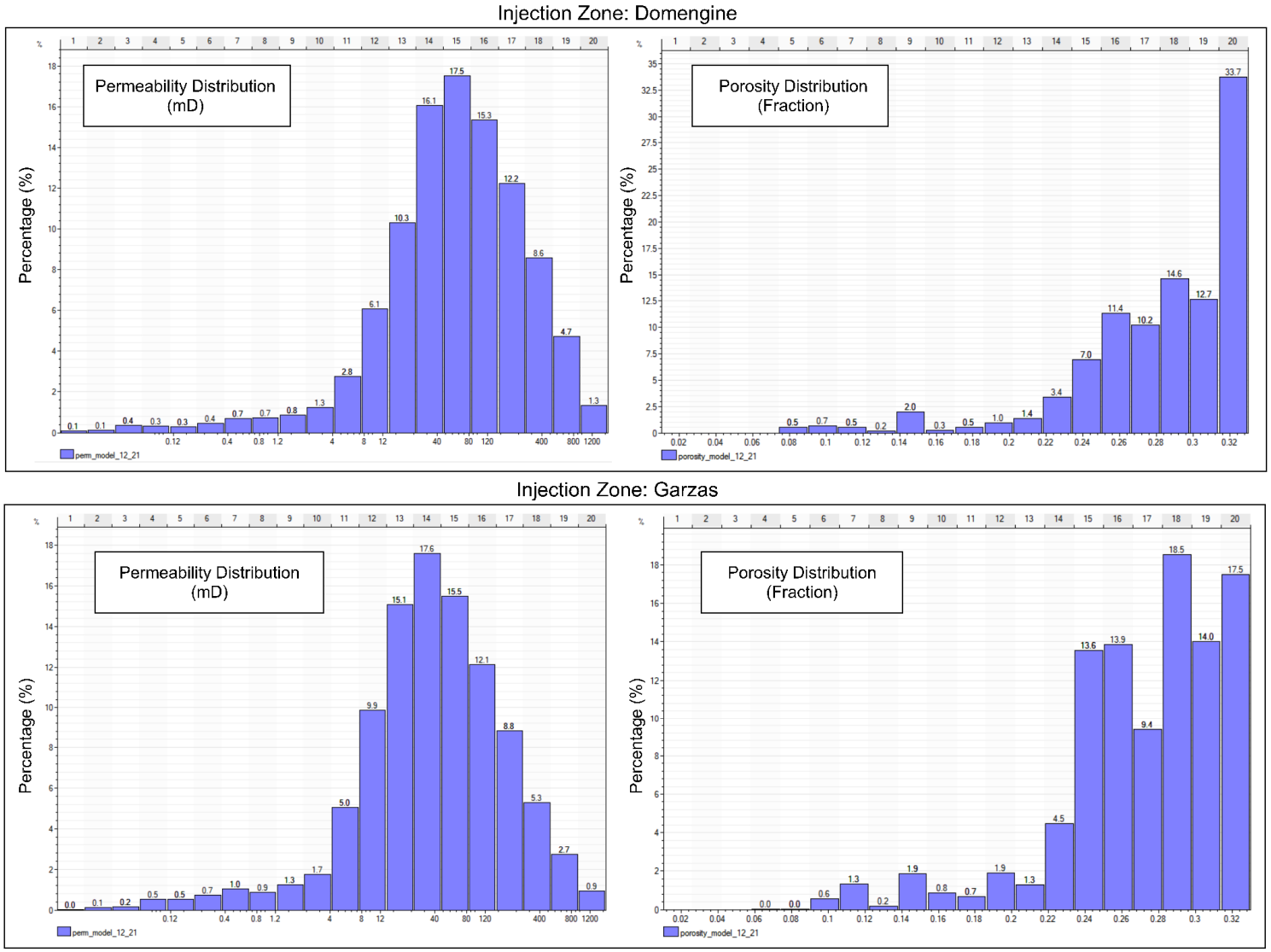

Figure 3.8(a). Domengine and Garzas Injection Zones porosity and permeability distribution used in static model.

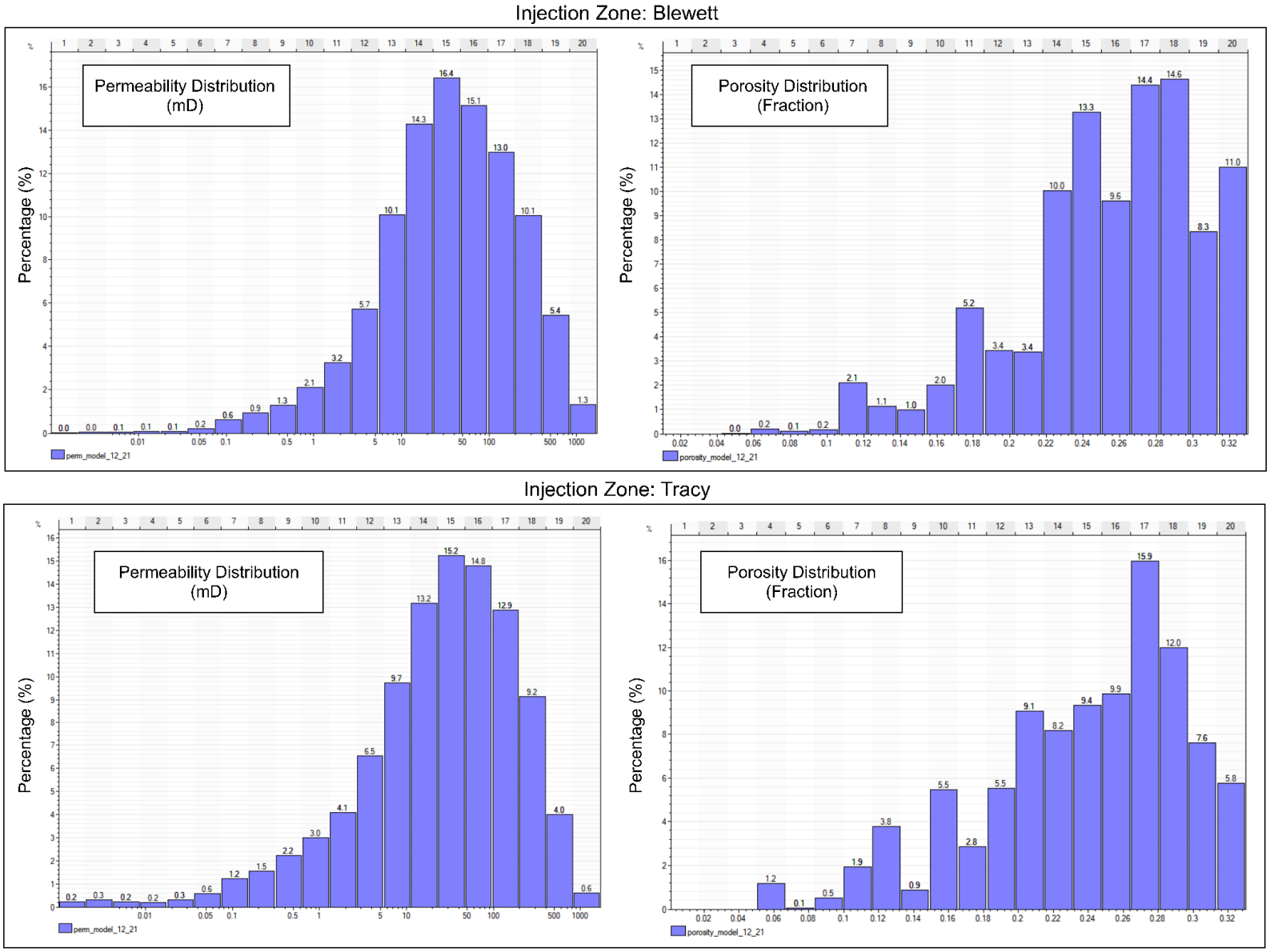

Figure 3.8(b). Blewett and Tracy Injection Zones porosity and permeability distribution used in static model.

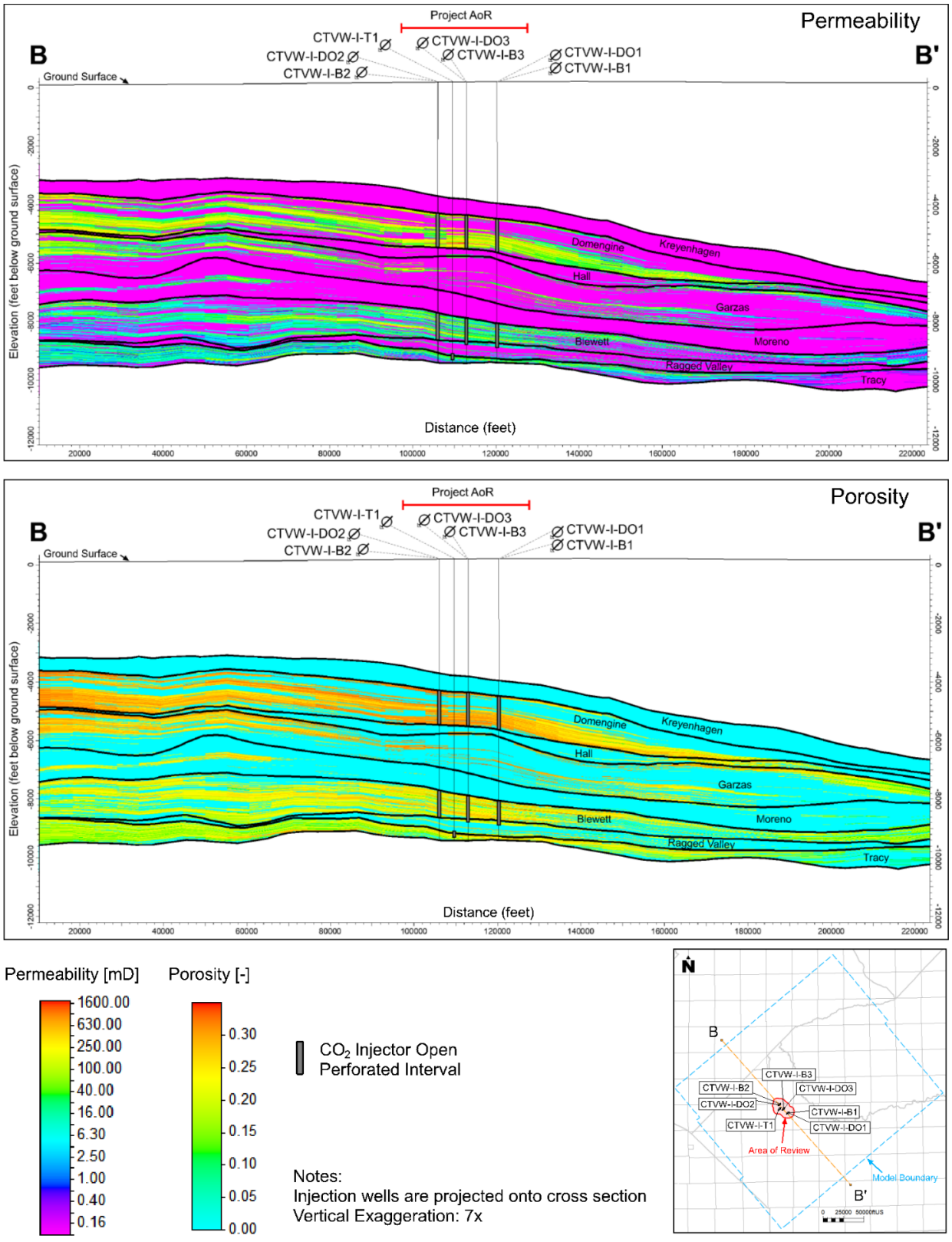

Figure 3.9. Section B-B' through the static grid showing distribution of porosity and permeability in Injection and Confining Zones.

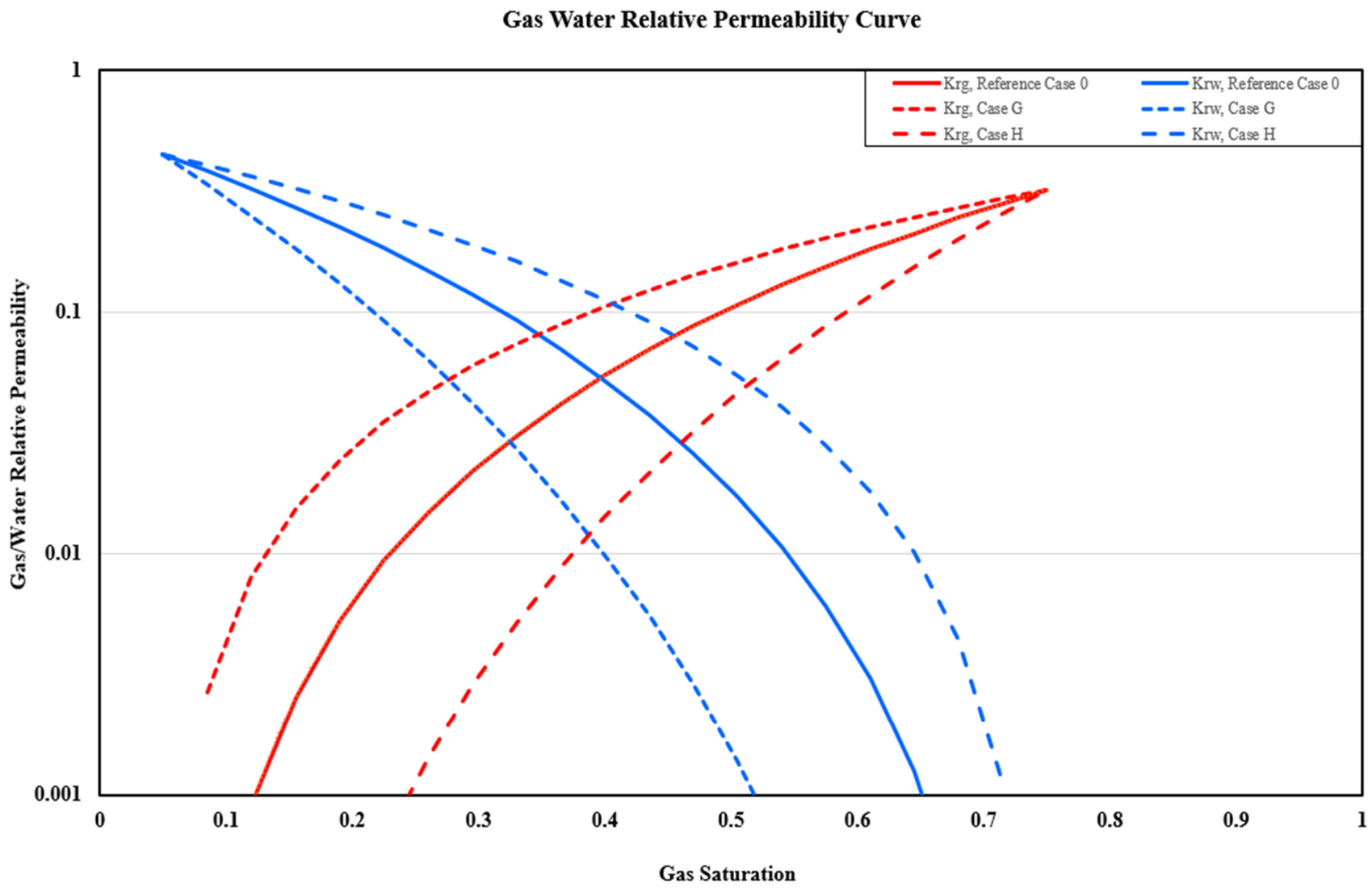

Figure 3.10. Relative permeability curves for Gas-Water system.

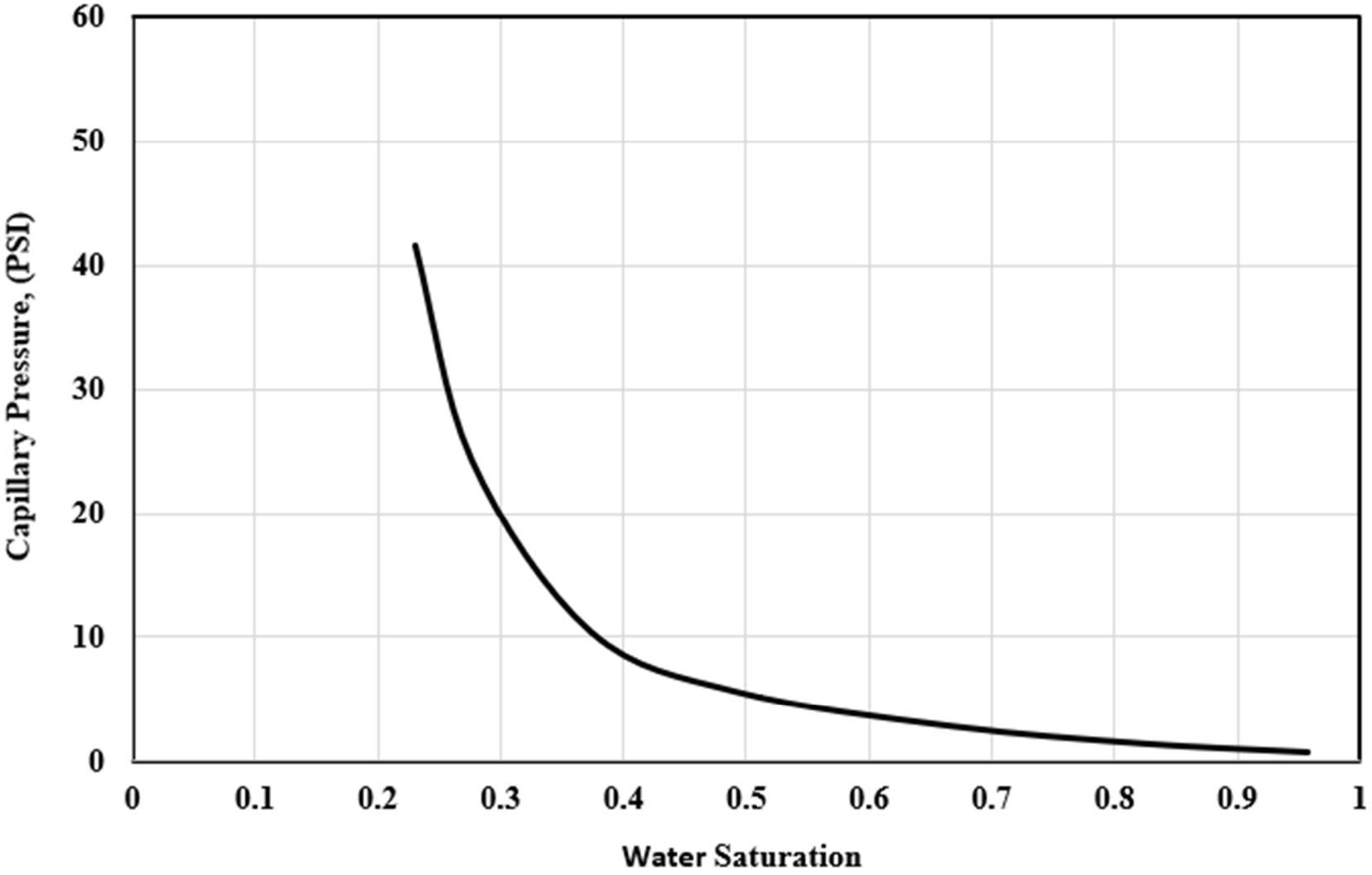

Figure 3.11. Capillary pressure curve.

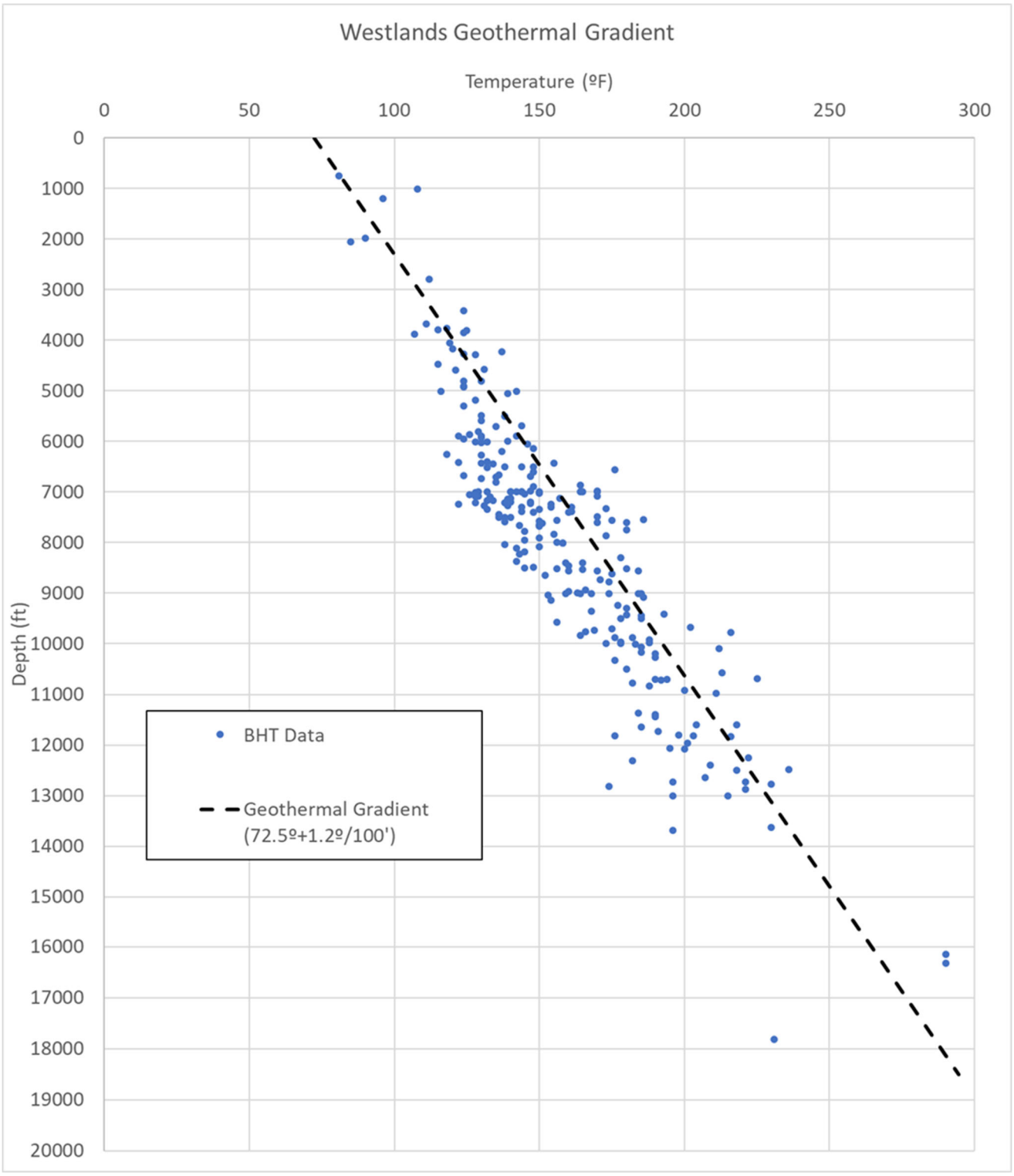

Figure 3.12(a). Geothermal gradient used for model initial conditions. The gradient is based on 248 bottom-hole temperature datapoints from individual logging runs.

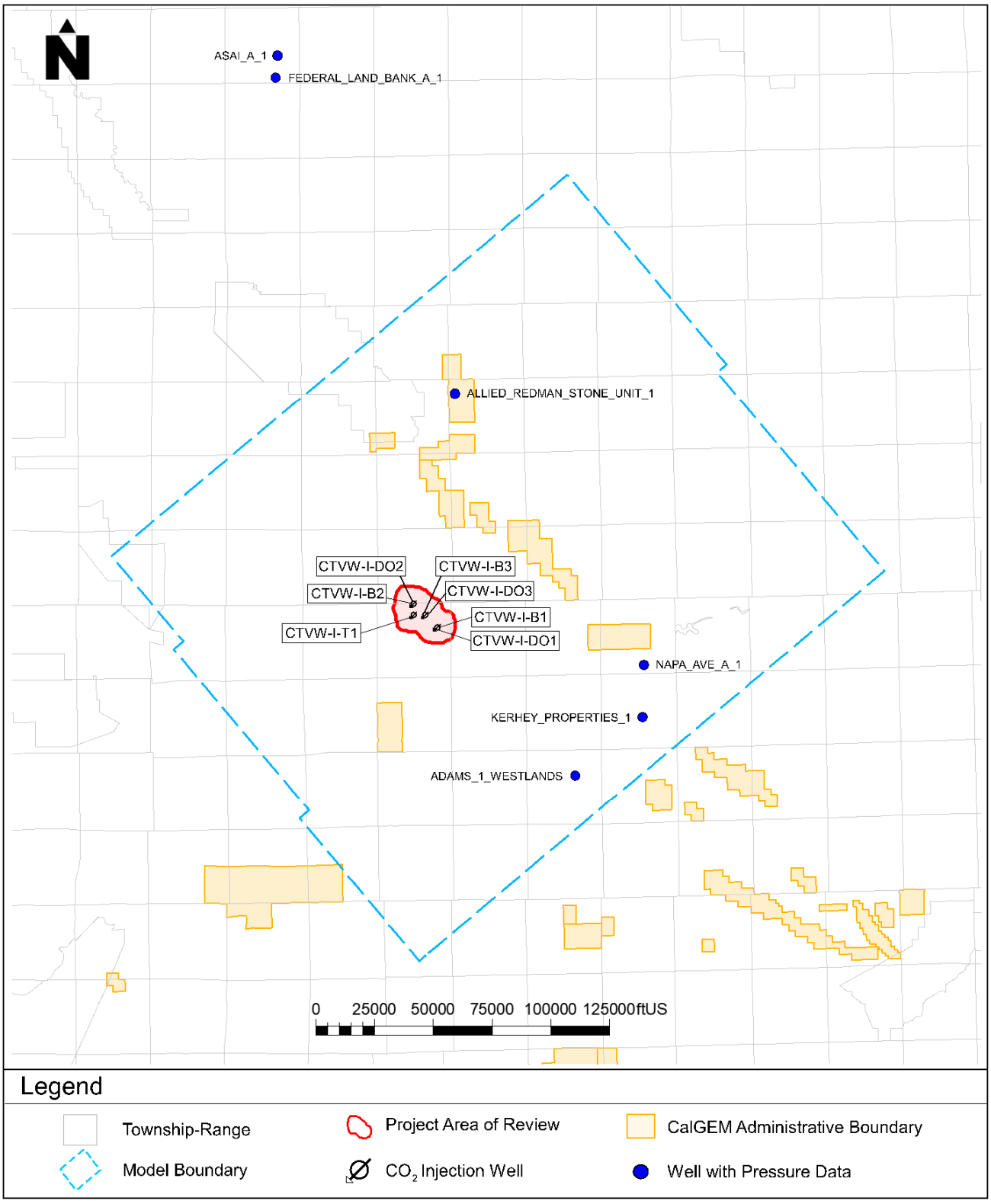

Figure 3.12(b). Well locations with RFT pressure data.

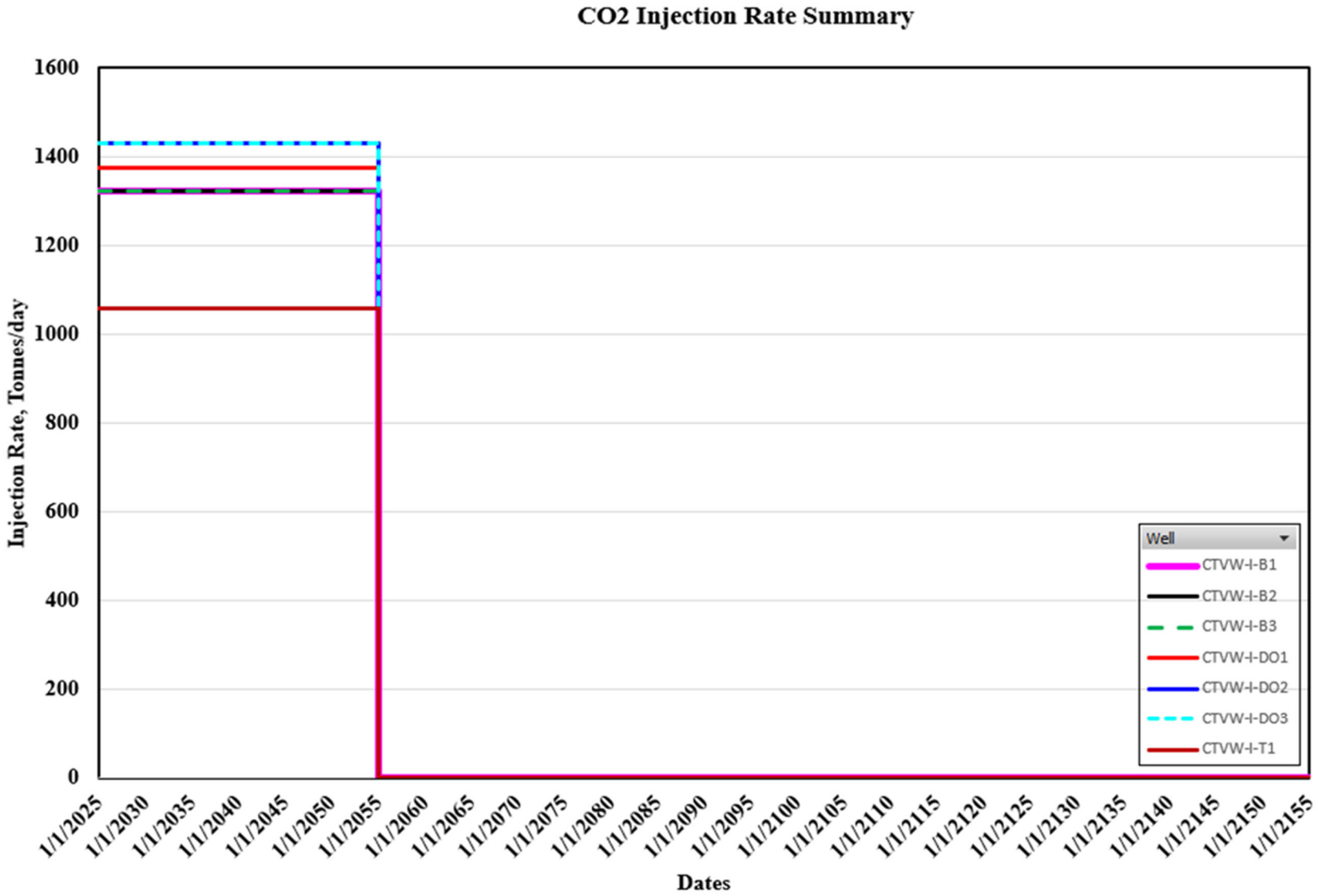

Figure 3.13. Base case CO_2 injection rate vs. time for each injector.

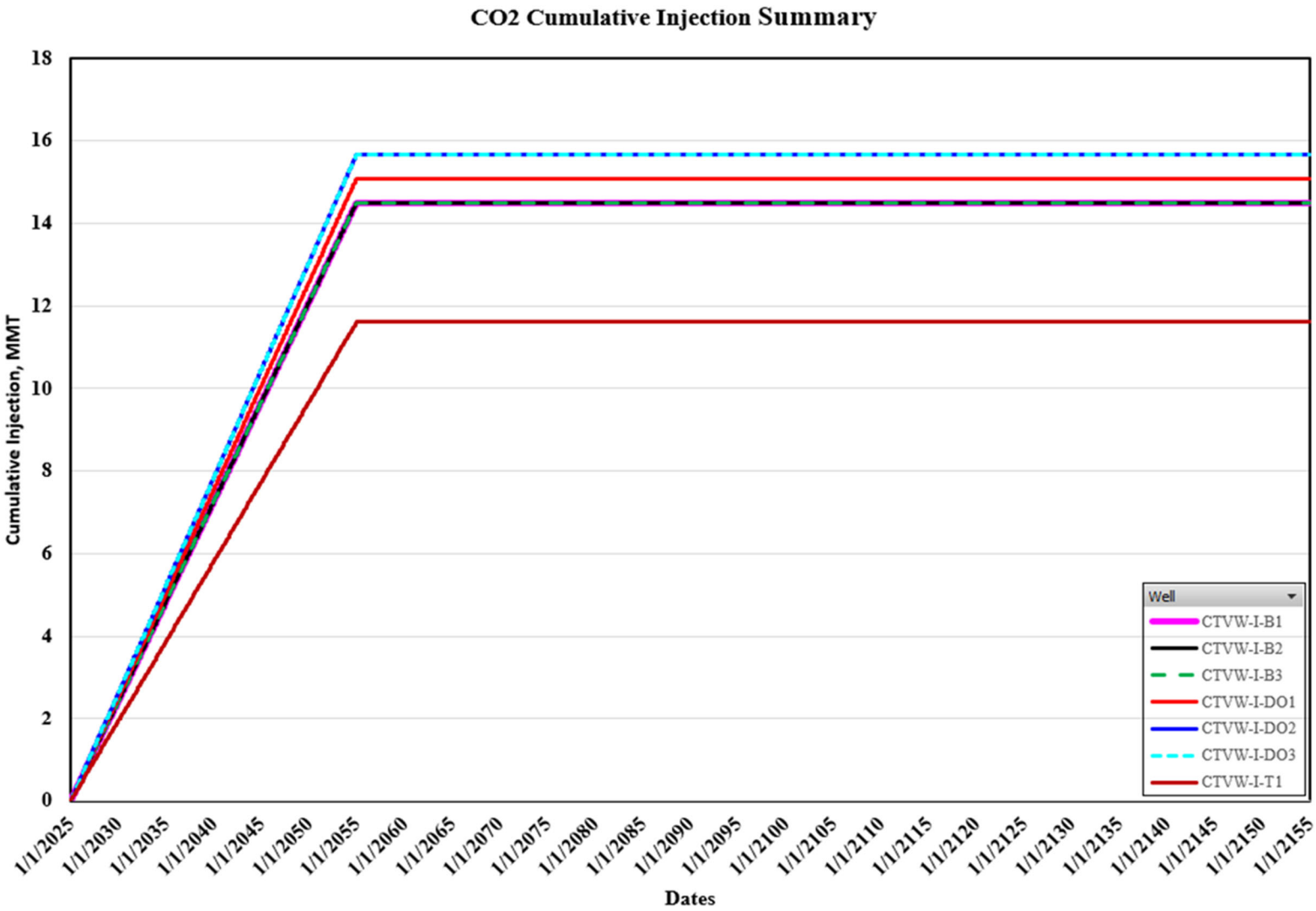

Figure 3.14. Base case CO_2 cumulative CO_2 injection vs. time for each injector.

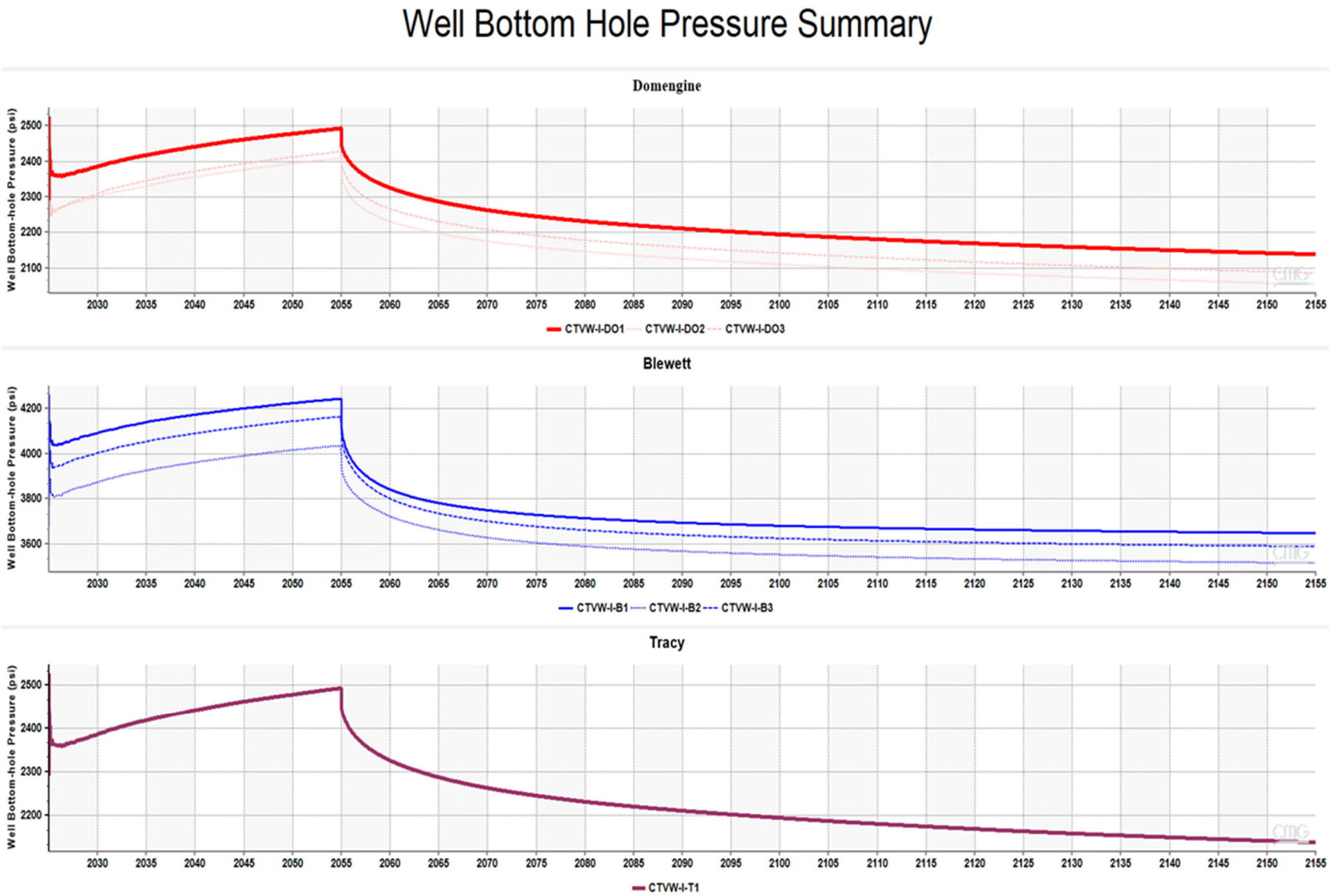

Figure 3.15. Base case CO_2 well bottom-hole pressure.

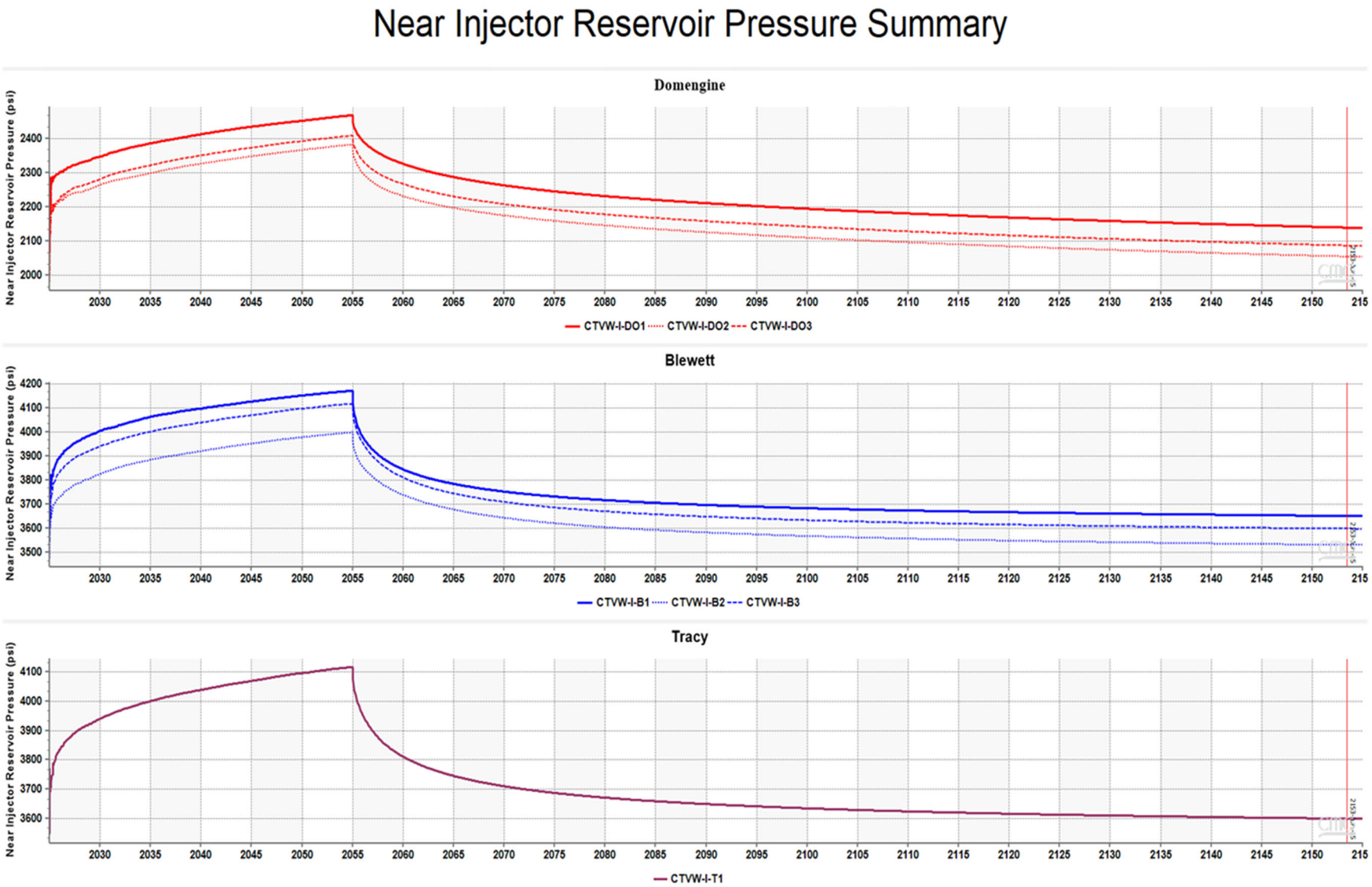

Figure 3.16. Base case CO_2 near injectors reservoir pressure for each injector.

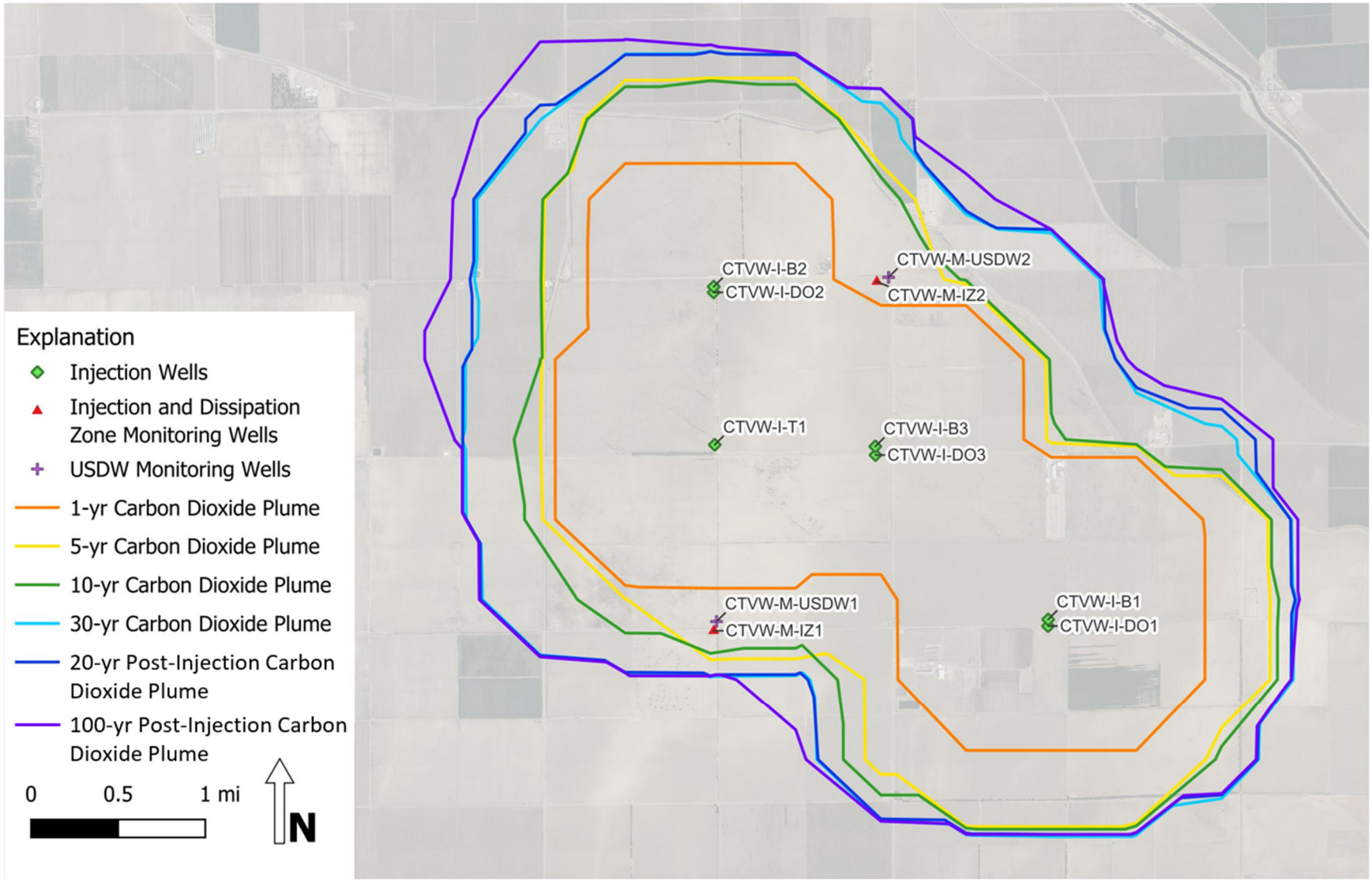

Figure 4.1. Injection Zone plume development through time: 1-year, 5-year, 10-year, 30-year (end of injection), 20-year, and 100-year post-injection.

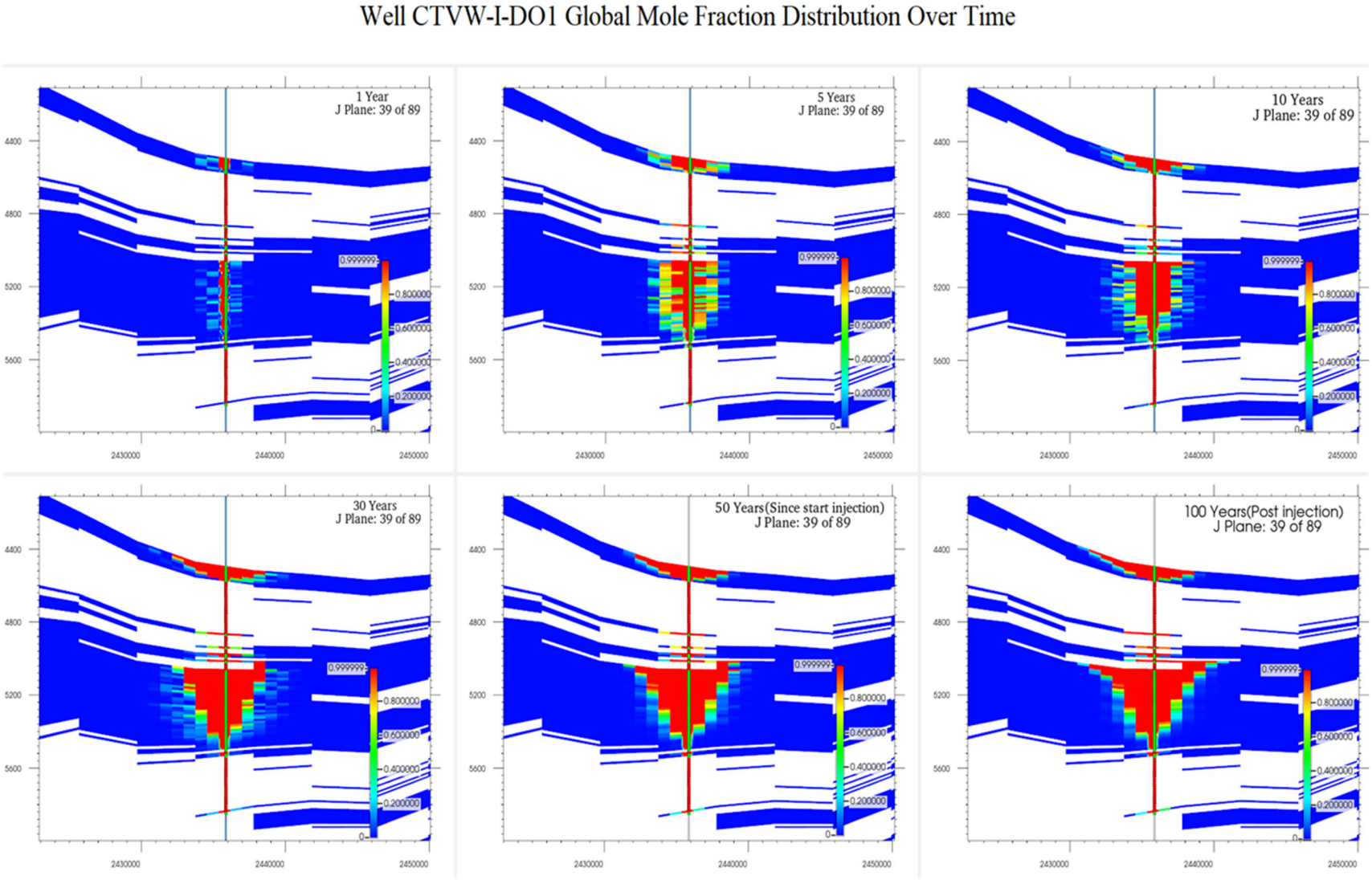

Figure 4.2(a). Base case CO_2 well CTVW-I-DO1 CO_2 global mole fraction distribution at 1 year, 5 years, 10 years, 30 years (projected end of injection), 50 years (since start of injection), and 100 years post-injection.

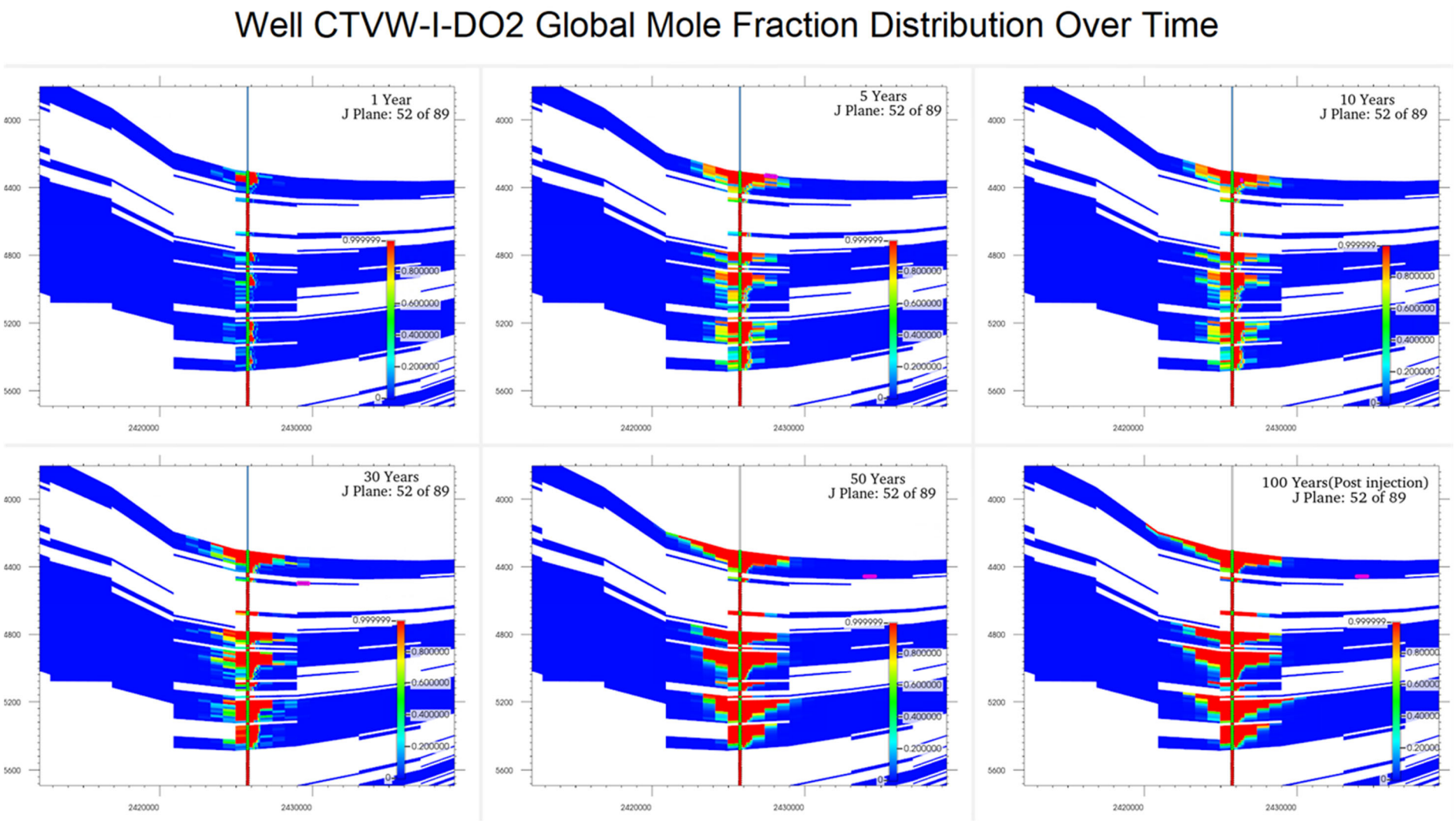

Figure 4.2(b). Base case CO_2 well CTVW-I-DO2 CO_2 global mole fraction distribution at 1 year, 5 years, 10 years, 30 years (projected end of injection), 50 years (since start of injection), and 100 years post-injection.

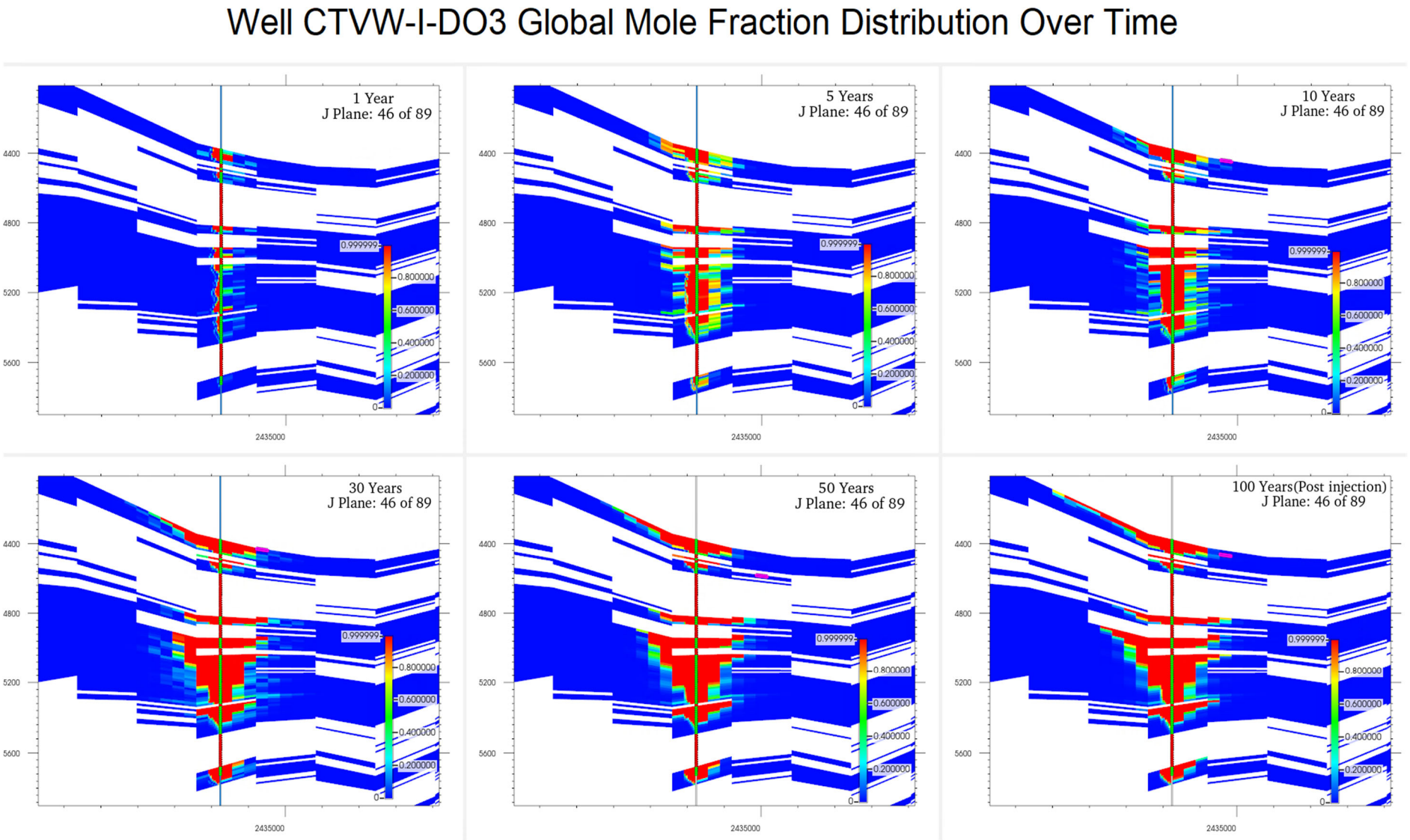

Figure 4.2(c). Base case CO_2 well CTVW-I-DO3 CO_2 global mole fraction distribution at 1 year, 5 years, 10 years, 30 years (projected end of injection), 50 years (since start of injection), and 100 years post-injection.

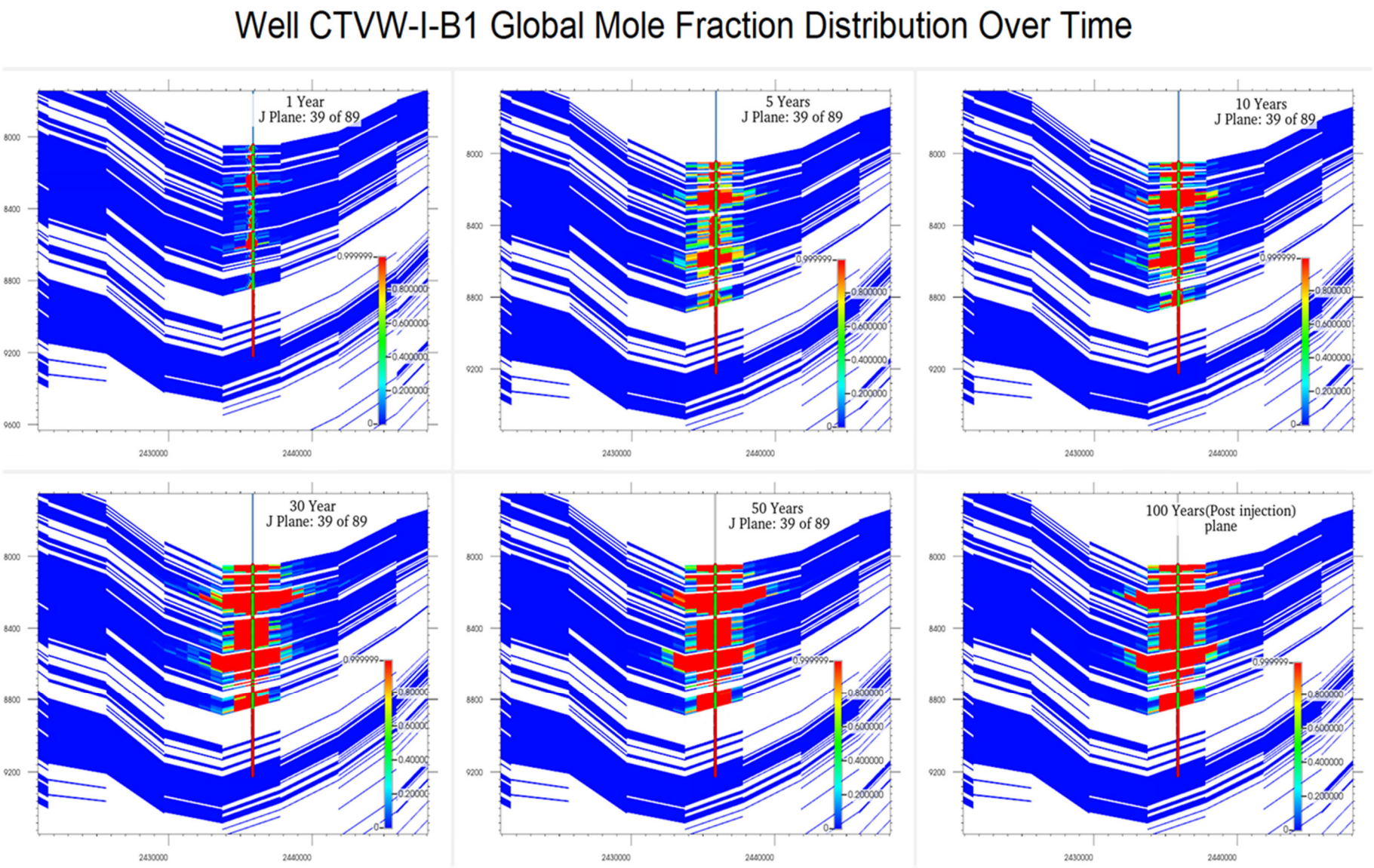

Figure 4.2(d). Base case CO_2 well CTVW-I-B1 CO_2 global mole fraction distribution at 1 year, 5 years, 10 years, 30 years (projected end of injection), 50 years (since start of injection), and 100 years post-injection.

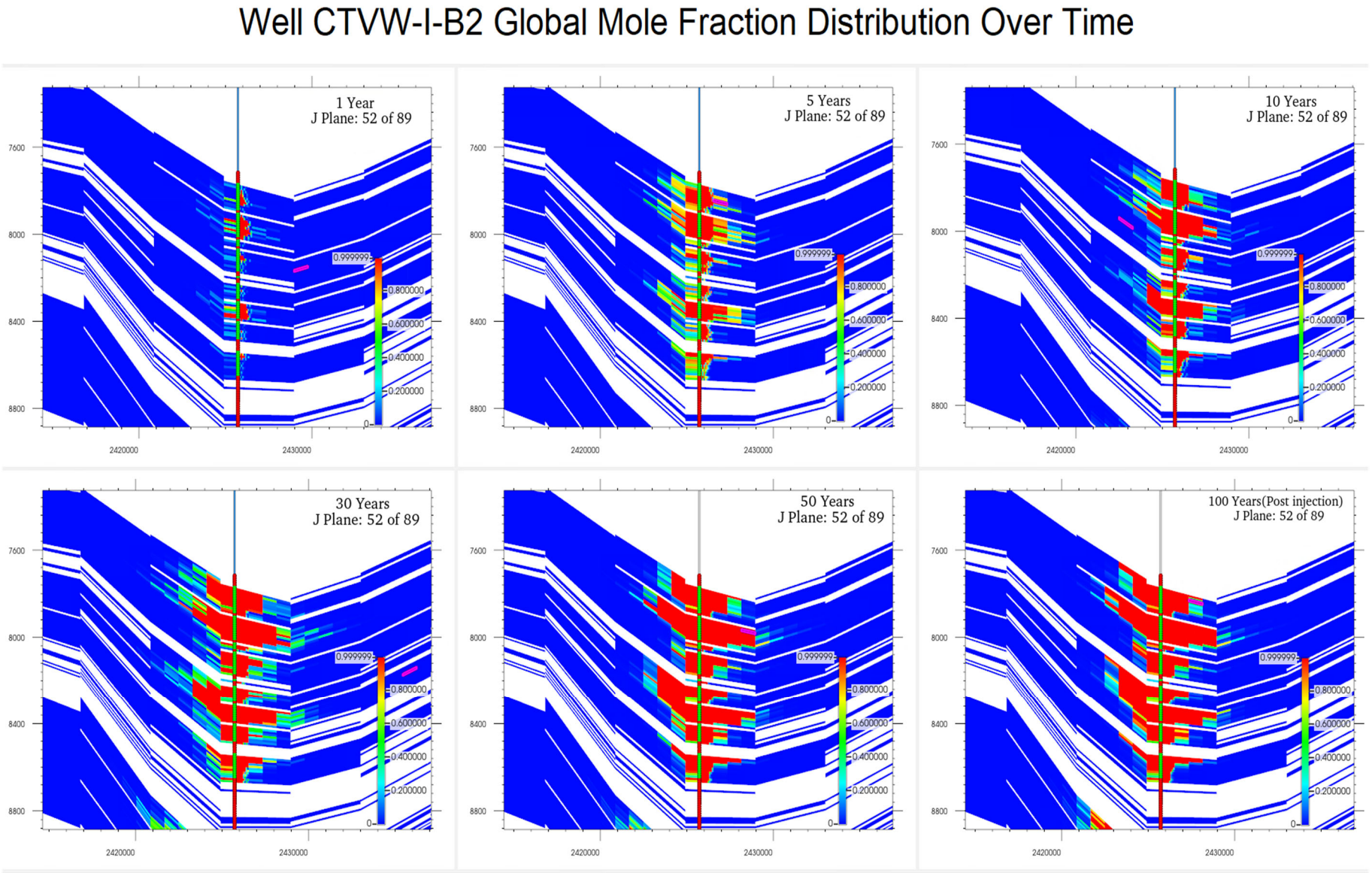

Figure 4.2(e). Base case CO_2 well CTVW-I-B2 CO_2 global mole fraction distribution at 1 year, 5 years, 10 years, 30 years (projected end of injection), 50 years (since start of injection), and 100 years post-injection.

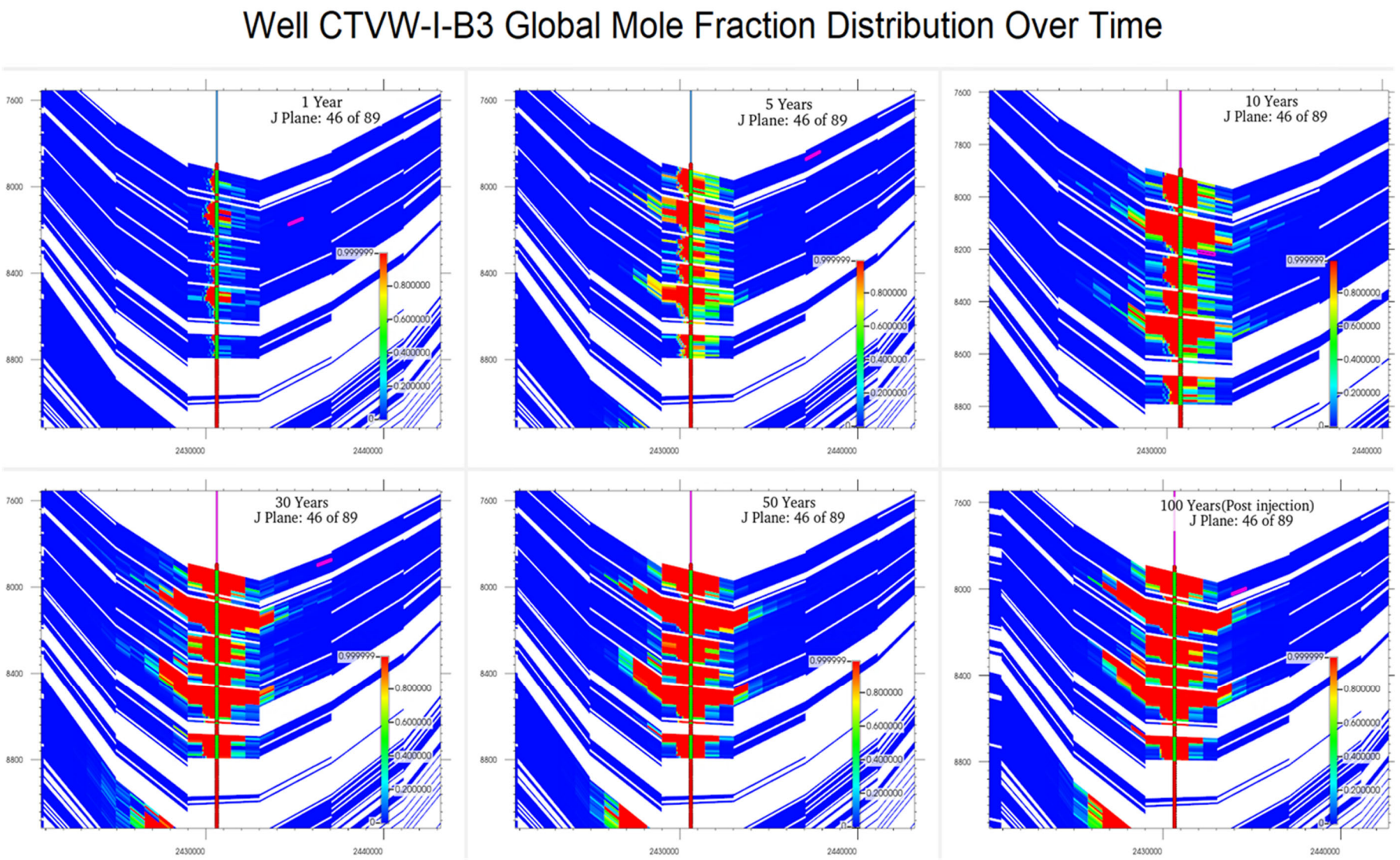

Figure 4.2(f). Base case CO_2 well CTVW-I-B3 CO_2 global mole fraction distribution at 1 year, 5 years, 10 years, 30 years (projected end of injection), 50 years (since start of injection), and 100 years post-injection.

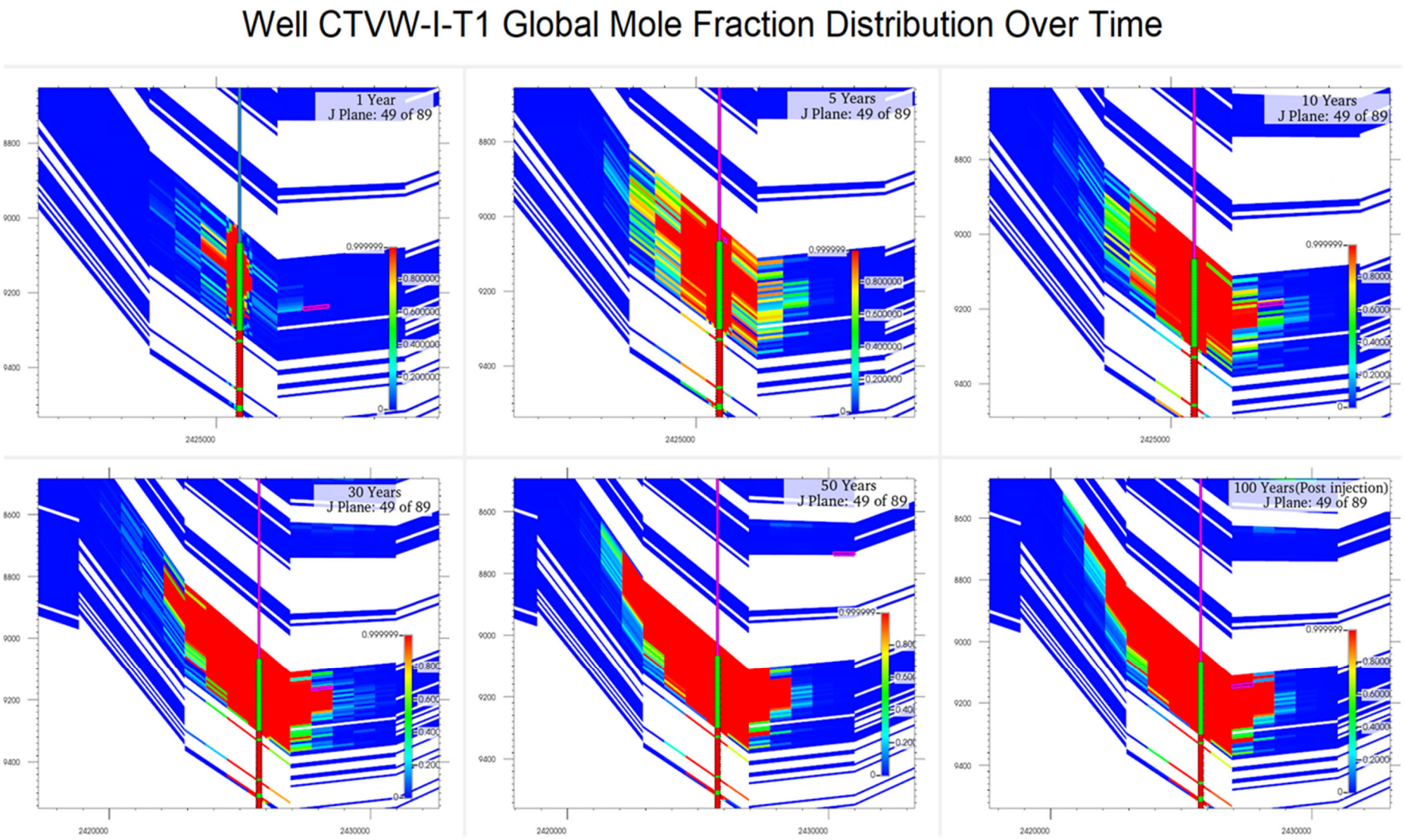

Figure 4.2(g). Base case CO_2 well CTVW-I-T1 CO_2 global mole fraction distribution at 1 year, 5 years, 10 years, 30 years (projected end of injection), 50 years (since start of injection), and 100 years post-injection.

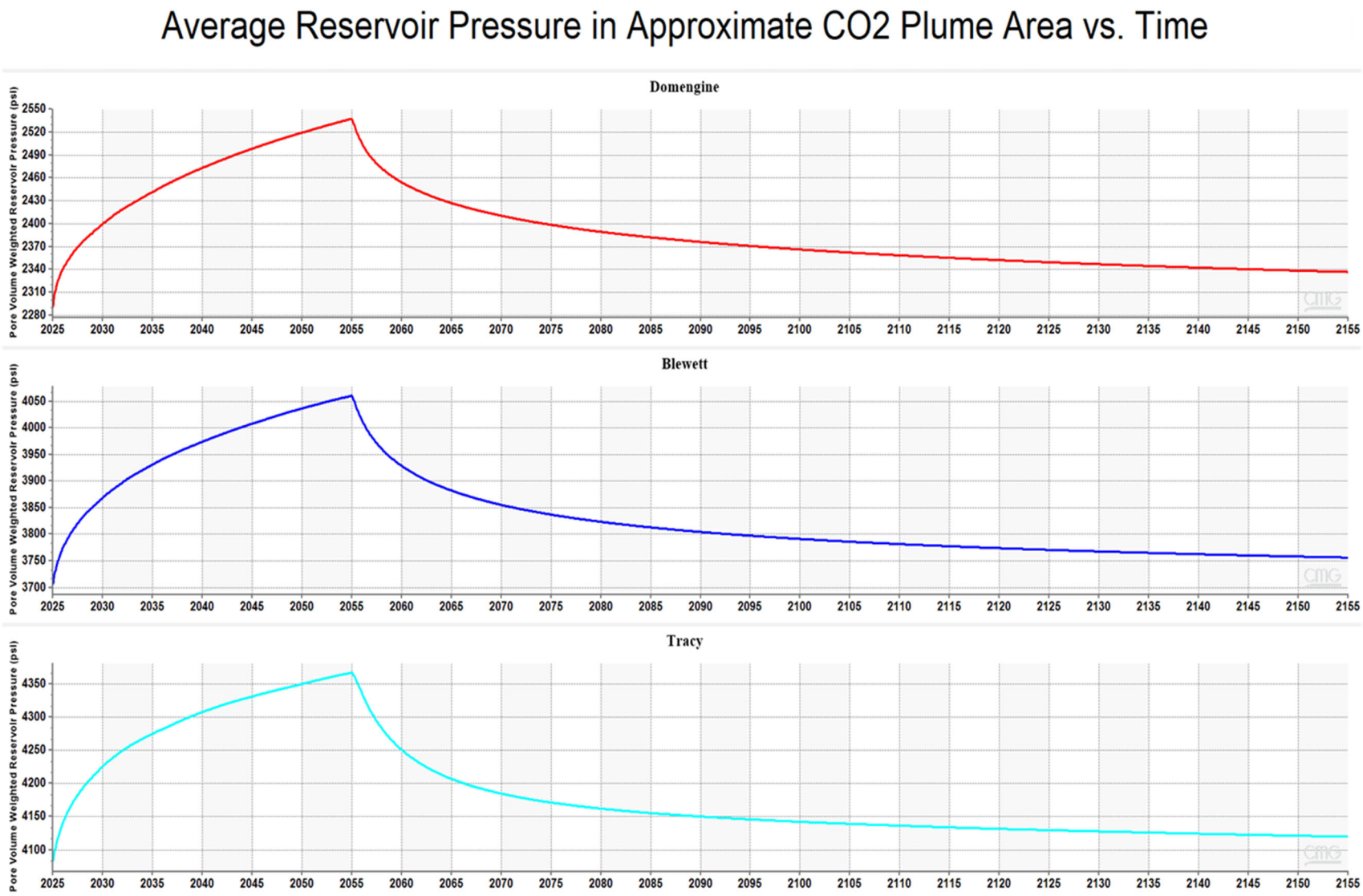

Figure 4.3(a). Base case CO_2 Average reservoir pressure within approximate plume area.

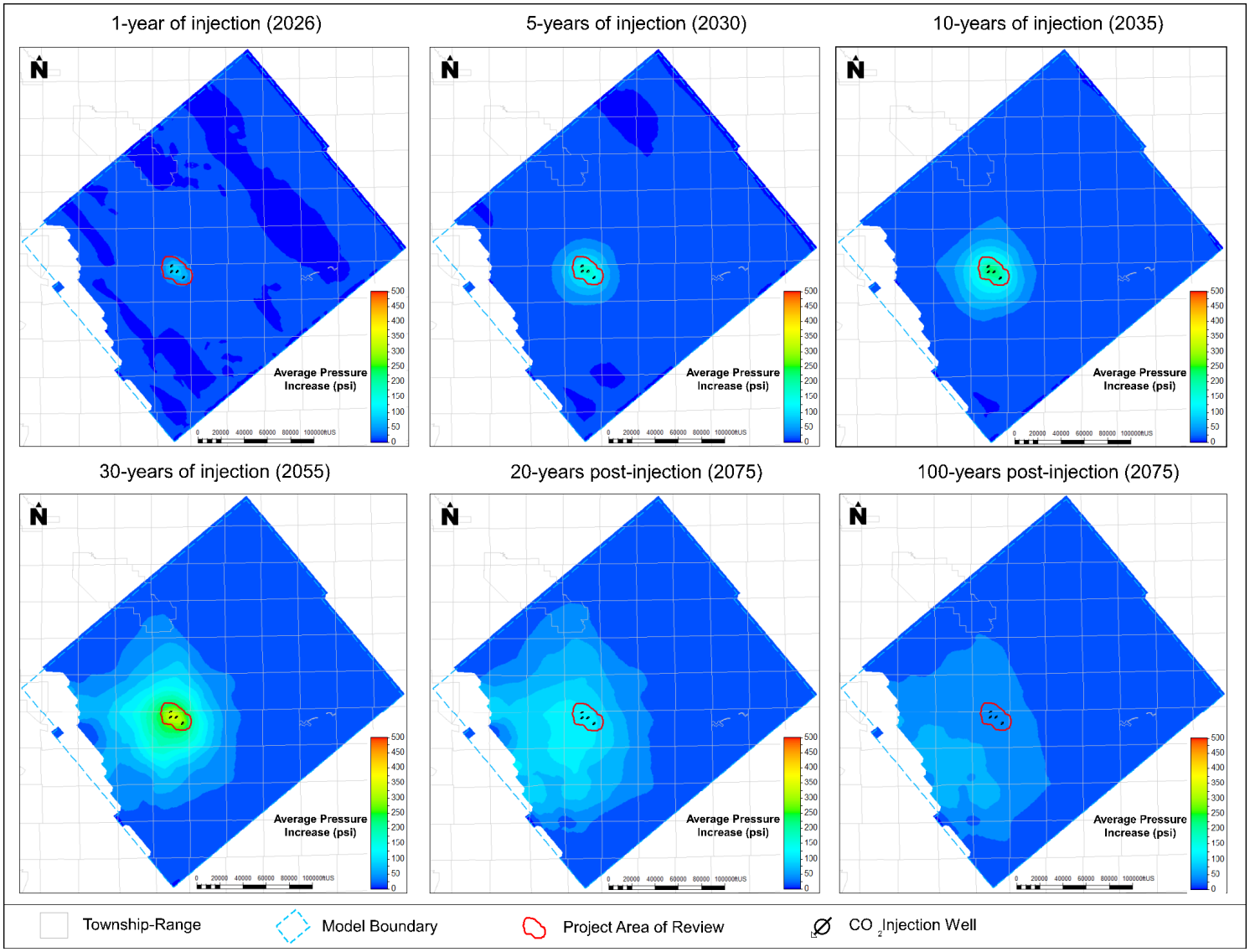

Figure 4.3(b). Maximum injection-induced pressure through time at the uppermost injection layer (directly below the top confining layer).

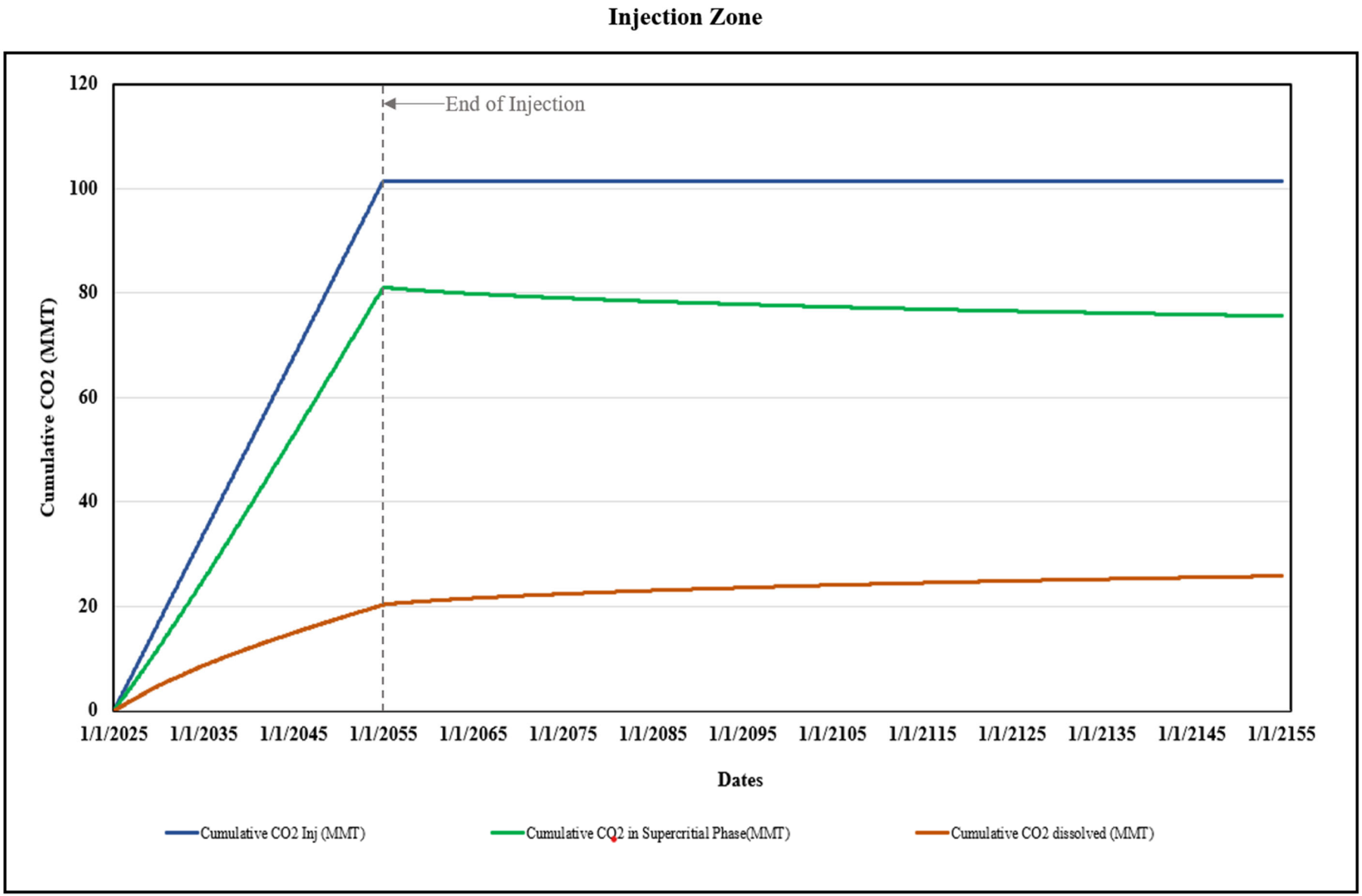

Figure 4.4 CO_2 storage mechanisms in the reservoir.

Injection Zones

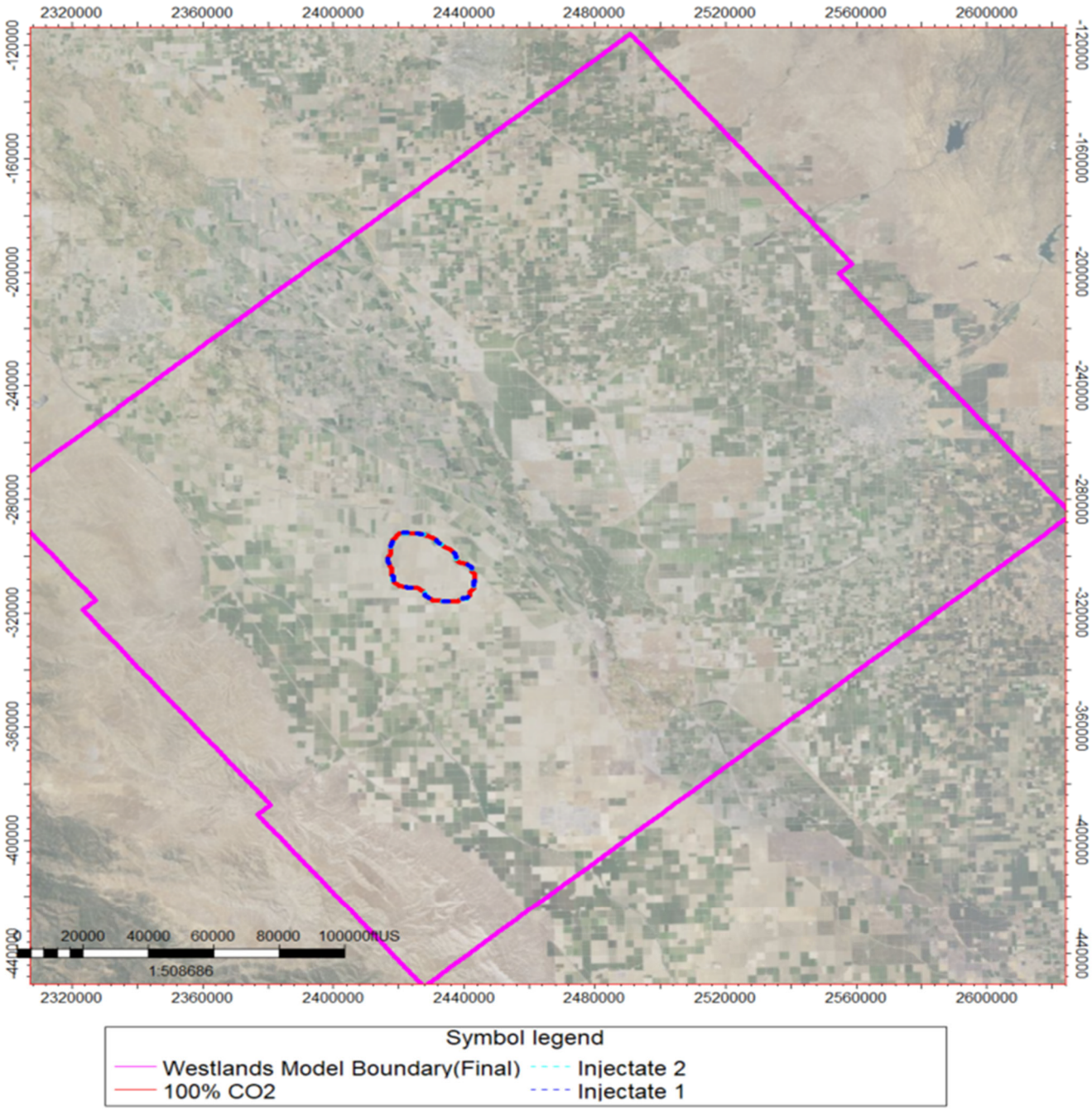

Figure 4.5. CO_2 plume boundary for Injectate 1 case (light blue dash line), Injectate 2 case (light green dashed line), and Base case CO_2 (red). Larger pink outline is the model boundary. Minimal differences in plume boundaries are observed among the three cases, with boundaries generally overlying each other.

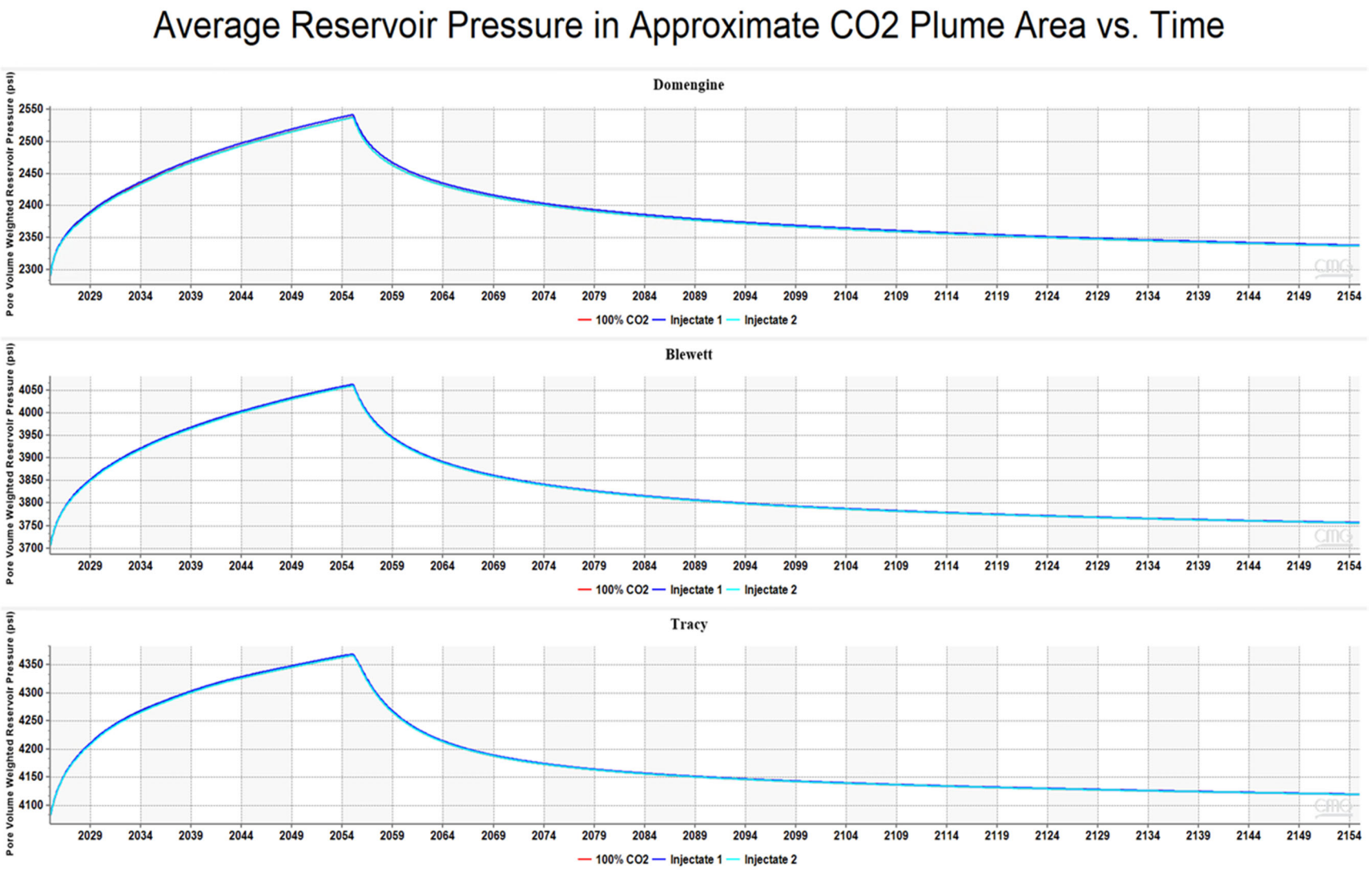

Figure 4.6. Average reservoir pressure within approximate plume area for Injectate 1, Injectate 2, and Base case (100% CO_2). Pressure trends for all cases plot almost on top of each other.

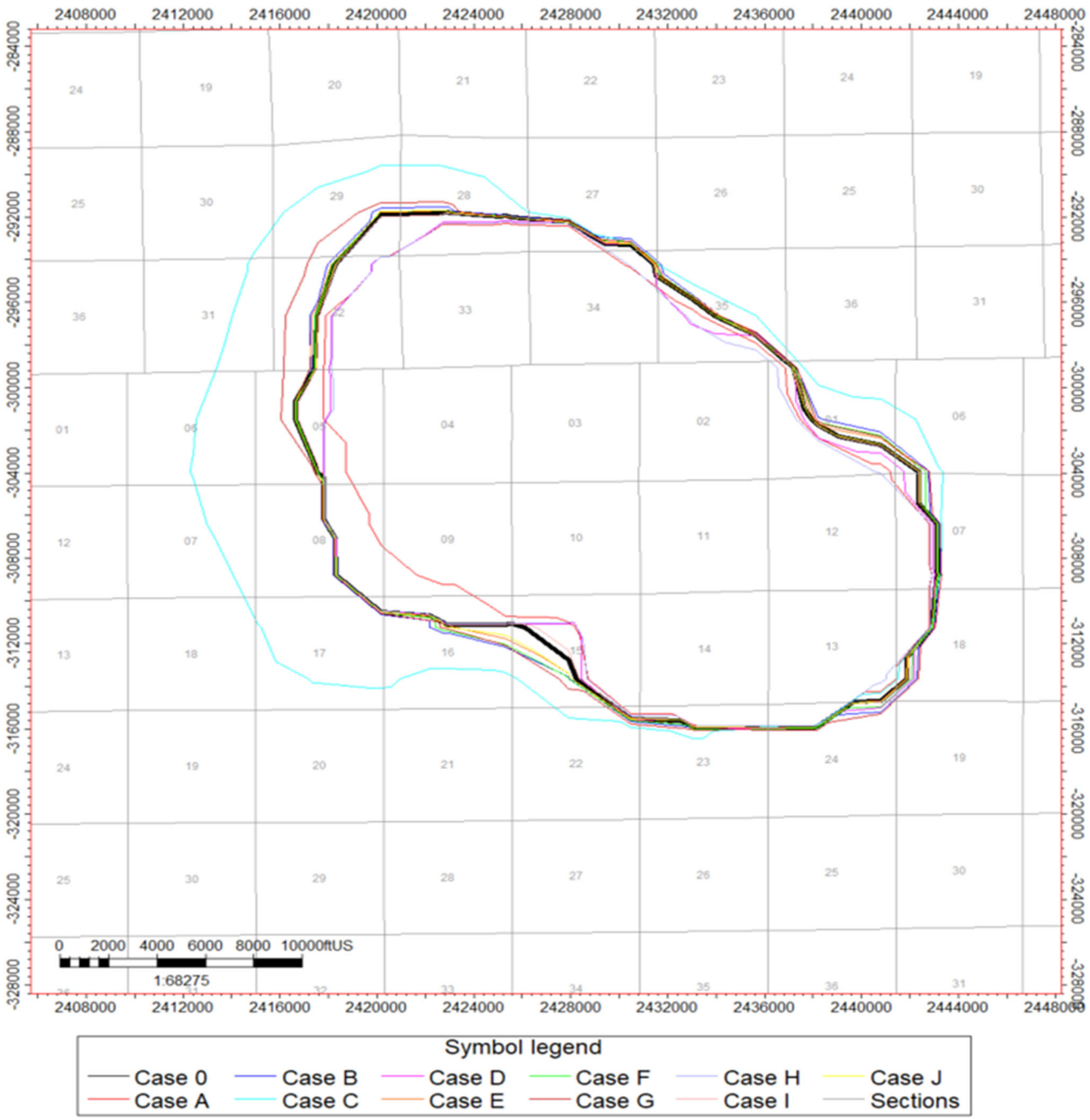

Figure 4.7. Submitted plume boundary and CO_2 plume outlines for CASE A to CASE J vs. reference case (Case 0) with 100% CO_2. Larger red outline is model boundary. Minimal difference in plume boundaries for most scenarios except for Case C with extreme parameters. CO_2 plume is defined by 0.01 CO_2 global mole fraction cutoff 100 years post-injection. See **Table 4.1** for scenario descriptions.

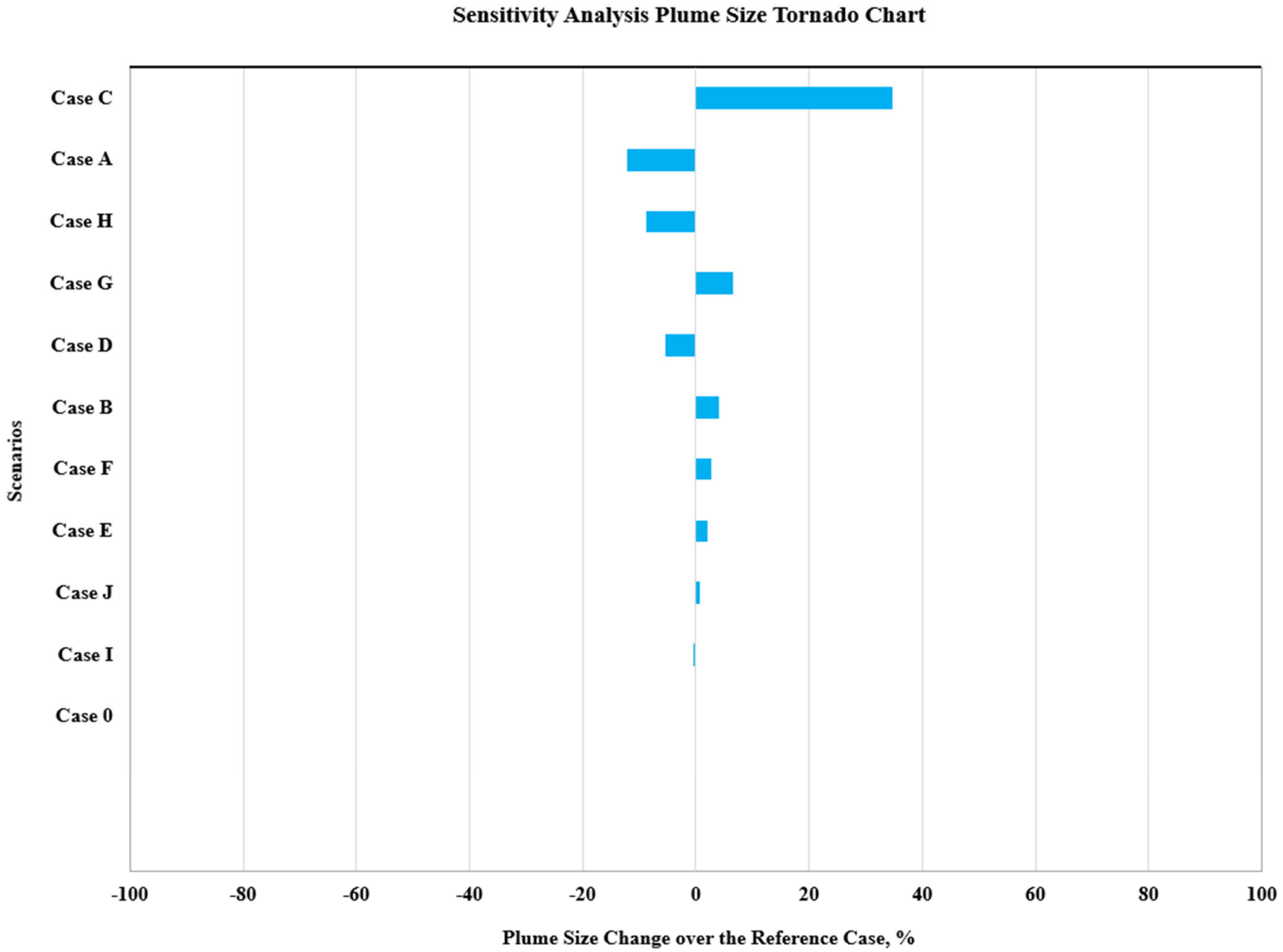

Figure 4.8. Injection Zone, Sensitivity analysis Tornado chart for plume size. See **Table 4.1** for scenario descriptions.

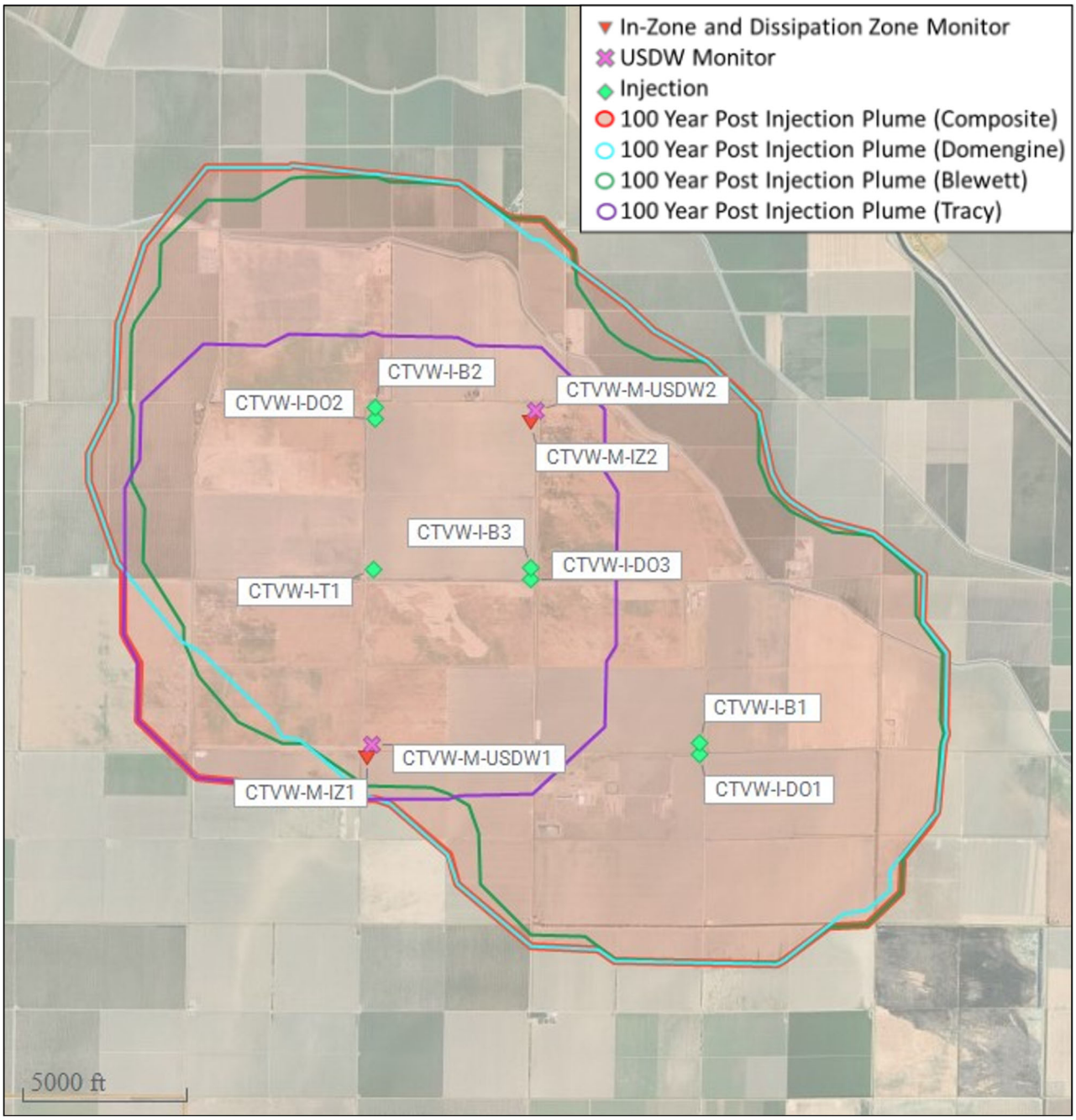

Figure 4.9. Location of injection and monitoring wells.

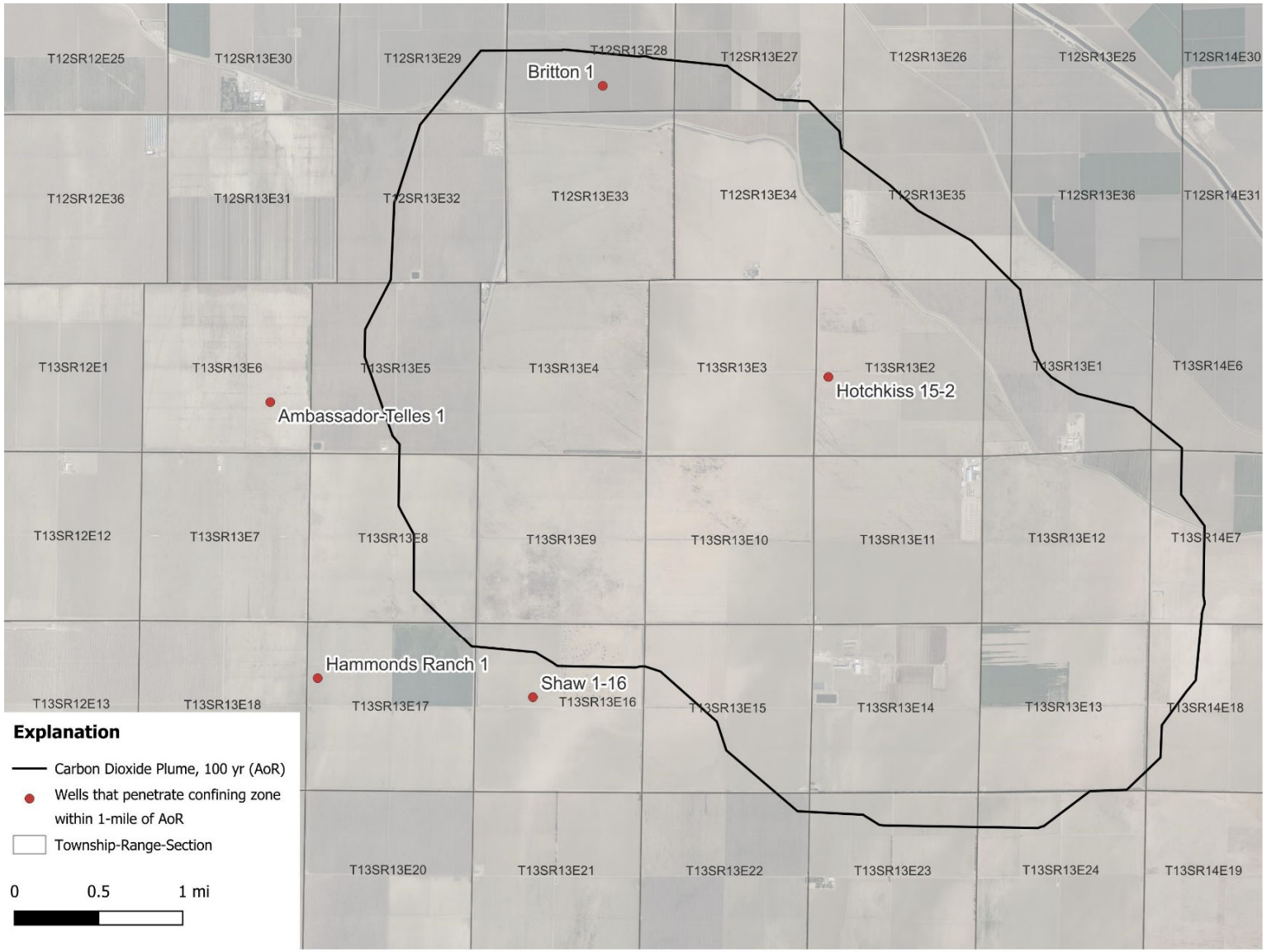

Figure 5.1. Wells penetrating Kreyenhagen Shale confining layer within 1 mile of the AoR. Two wells are identified as falling within the AoR and for corrective action.

Tables

Table 3.1. Model Domain Information

Coordinate System	State Plane		
Horizontal Datum	North American Datum (NAD) 27		
Coordinate System Units	Feet		
Zone	Zone 2		
FIPSZONE	0402	ADSZONE	3301
Coordinate of X min	2,296,689,56	Coordinate of X max	2,625,941.81
Coordinate of Y min	-451,611.37	Coordinate of Y max	-116,082.14
Elevation of Bottom of Domain	-14,709.18	Elevation of Top of Domain	-50

Table 3.2. Carter-Tracy Aquifer Property

Injection Zone	Net Thickness (feet)	Porosity fraction	Permeability (millidarcy)	Effective reservoir Radius (feet)	Angle, a fraction of a circle	Ratio of the aquifer's external radius to the effective reservoir radius
Domengine	316	0.2845	141	129,208	0.25	2.04
Garzas	345	0.2718	102	129,208	0.25	2.04
Blewett	376	0.2549	111	129,208	0.25	2.04
Tracy	507	0.2383	90	129,208	0.25	2.04

Table 3.3. Initial Conditions

Parameter	Injection Zone	Value	Units	Corresponding Elevation (ft msl)	Data Source
Temperature	Domengine	135°	Fahrenheit	4,975	Depth-dependent and based on a temperature gradient of 0.012° F/foot, as calculated from bottom hole temperature logged in wells in the study area with directional surveys, and a surface temperature of 72.5°F
	Garzas	155°		6,671	
	Blewett	177°		8,487	
	Tracy	192°		9,774	
Formation Pressure	Domengine	2,271	Pounds per square inch	4,975	Hydrostatic, assumed normal pressure aquifer
	Garzas	3,015		6,671	
	Blewett	3,812		8,487	
	Tracy	4,377		9,774	
Salinity	Domengine	20,700	Parts per million	4,975	Attachment A, Section 2.8.2.3
	Garzas	20,700		6,671	Attachment A, Section 2.8.2.4
	Blewett	20,700		8,487	Attachment A, Section 2.8.2.5
	Tracy	21,100		9,774	Attachment A, Section 2.8.2.6

Table 3.4. Operational Details

Operating Information	Injection Well CTVW-I-DO1 Domengine	Injection Well CTVW-I-DO2 Domengine	Injection Well CTVW-I-DO3 Domengine	Injection Well CTVW-I-B1 Blewett	Injection Well CTVW-I-B2 Blewett	Injection Well CTVW-I-B3 Blewett	Injection Well CTVW-I-T1 Tracy
Location (global coordinates)	36.80749903 -120.5133076	36.83568421 -120.5473443	36.82215533 -120.5308907	36.80749903 -120.5133076	36.83568421 -120.5473443	36.82215533 -120.5308907	36.82251043 -120.547504253
Model coordinates (ft) X, Y	2435842.2, -309378.55	2425707.9, -299272.38	2430605.38, -304123.25	2435842.2, -309378.55	2425707.9, -299272.38	2430605.38, -304123.25	2425737.7, -304072.16
No. of perforated intervals	4	7	7	9	8	7	4
Perforated interval (ft MD/TVD/MSL) Top Bottom	4712/4712/4492 5761/5761/5541	4507/4507/4296 5686/5686/5475	4589/4589/4372 5716/5716/5499	8274/8274/8054 9084/9084/8864	7913/7913/7702 8858/8858/8647	8102/8102/7885 9009/9009/8792	9269/9269/9048 9501/9501/9280
Casing diameter (in.)	7	7	7	7	7	7	7
Modeled injection period Start End	01/01/2025 01/01/2055	01/01/2025 01/01/2055	01/01/2025 01/01/2055	01/01/2025 01/01/2055	01/01/2025 01/01/2055	01/01/2025 01/01/2055	01/01/2025 01/01/2055
Modeled Injection duration (years)	30	30	30	30	30	30	30
Modeled Injection rate (t/day)*	1376.8	1429.7	1429.7	1323.8	1323.8	1323.8	1059.0
Modeled CO_2 Injected (MMT)	15.1	15.7	15.7	14.5	14.5	14.5	11.6

*If planned injection rates change year to year, add rows to reflect this difference, and include an average injection rate per year (or interval if applicable).

Table 3.5. Injection Pressure Details

Injection Pressure Details	Injection Well CTVW-I-DO1 Domengine	Injection Well CTVW-I-DO2 Domengine	Injection Well CTVW-I-DO3 Domengine	Injection Well CTVW-I-B1 Blewett	Injection Well CTVW-I-B2 Blewett	Injection Well CTVW-I-B3 Blewett	Injection Well CTVW-I-T1 Tracy
Fracture gradient (psi/ft)	0.80	0.80	0.80	0.80	0.80	0.80	0.80
Maximum allowable downhole injection pressure (90% of fracture pressure) (psi)	3,393	3,245	3,304	5,957	5,697	5,833	6,674
Elevation corresponding to maximum injection pressure (ft TVD)	4,712	4,507	4,589	8,274	7,913	8,102	9,269
Elevation at the top of the perforated interval (ft TVD)	4,712	4,507	4,589	8,274	7,913	8,102	9,269
Planned injection pressure (psi) / gradient (psi/ft) at top of perforations	2,343/ 0.4971	2,250/ 0.4993	2,267/ 0.4939	4,025/ 0.4865	3,816/ 0.4822	3,896/ 0.4809	4,727/ 0.5100

Table 3.6. Injectate Compositions

Component	Injectate 1 (Mass %)	Injectate 2 (Mass %)
CO_2	99.21%	99.88%
H_2	0.05%	0.01%
N_2	0.64%	0.00%
H_2O	0.02%	0.00%
CO	0.03%	0.00%
Ar	0.03%	0.00%
O_2	0.00%	0.00%
SO_2+SO_3	0.00%	0.00%
H_2S	0.00%	0.01%
CH_4	0.00%	0.04%
NOx	0.00%	0.00%
NH_3	0.00%	0.00%
C_2H_6	0.00%	0.05%
Ethylene	0.00%	0.00%
Total	100.00%	100.00%

Table 3.7. Injectate Concentration Limits

Component	Mol% Limit
CO_2	> 96%
H_2	< 1.00%
N_2	< 3.00%

Table 4.1. Simulation Sensitivity Scenarios

Case Name	Description	Reference	Perturbation
Case 0	Base case		NA
Case A	Increased porosity based on 10th percentile of measured values	1, multiplier	1.24, multiplier
Case B	Reduced porosity based on 90th percentile of measured values	1, multiplier	0.88, multiplier
Case C	Increase permeability by multiplier transform by 3; maintain anisotropy ratio	1, multiplier	3, multiplier
Case D	Reduce permeability by multiplier transform by 0.3; maintain anisotropy ratio	1, multiplier	0.3, multiplier
Case E	Reduced phase trapping by reduced residual gas saturation	S_{gr} = 0.25	S_{gr} = 0.05
Case F	Reduce phase trapping by increase residual water saturation	Sw_r = 0.25	Sw_r = 0.34
Case G	Change the shape for relative permeability	NG=2.55	NG=1.6
		NW=3.10	NW=5.5
Case H	Change the shape for relative permeability	NG=2.55	NG=4.5
		NW=3.10	NW=2.0
Case I	Capillary pressure increase 30%	1, multiplier	1.3, multiplier
Case J	Capillary pressure reduce 30%	1, multiplier	0.7, multiplier

Table 5.1. Wellbores in the AoR by Status

Status	Count
Active	0
Idle	0
Plugged and Abandoned	2
Total	2